OULU 2017
C 604

ACTA UNIVERSITATIS OULUENSIS

Petri Luoto

CO-PRIMARY MULTI-OPERATOR RESOURCE SHARING FOR SMALL CELL NETWORKS

UNIVERSITY OF OULU GRADUATE SCHOOL;
UNIVERSITY OF OULU,
FACULTY OF INFORMATION TECHNOLOGY AND ELECTRICAL ENGINEERING;
CENTRE FOR WIRELESS COMMUNICATIONS;
INFOTECH OULU

ACTA UNIVERSITATIS OULUENSIS
C Technica 604

PETRI LUOTO

CO-PRIMARY MULTI-OPERATOR RESOURCE SHARING FOR SMALL CELL NETWORKS

Academic dissertation to be presented with the assent of the Doctoral Training Committee of Technology and Natural Sciences of the University of Oulu for public defence in the OP auditorium (L10), Linnanmaa, on 16 March 2017, at 12 noon

UNIVERSITY OF OULU, OULU 2017

Acta Univ. Oul. C 604, 2017

Supervised by
Professor Matti Latva-aho
Docent Mehdi Bennis

Reviewed by
Professor Klaus Moessner
Doctor Emilio Calvanese Strinati

Opponent
Professor Babak H. Khalaj

ISBN 978-952-62-1496-2 (Paperback)
ISBN 978-952-62-1497-9 (PDF)

ISSN 0355-3213 (Printed)
ISSN 1796-2226 (Online)

Cover Design
Raimo Ahonen

JUVENES PRINT
TAMPERE 2017

Luoto, Petri, Co-primary multi-operator resource sharing for small cell networks.
University of Oulu Graduate School; University of Oulu, Faculty of Information Technology and Electrical Engineering; Centre for Wireless Communications; Infotech Oulu
Acta Univ. Oul. C 604, 2017
University of Oulu, P.O. Box 8000, FI-90014 University of Oulu, Finland

Abstract

The aim of this thesis is to devise novel co-primary spectrum sharing (CoPSS) methods for future fifth generation (5G) networks and beyond. The target is to improve data rates of small cell networks (SCNs) in which mobile network operators (MNOs) share their dedicated frequency spectrum (spectrum pooling) or a common spectrum (mutual renting). The performance of the proposed methods is assessed through extensive system-level simulations.

MNOs typically acquire exclusive usage rights for certain frequency bands and have little incentive to share spectrums with other operators. However, due to higher cost and spectrum scarcity at lower frequencies it is expected that efficient use of the spectrum in 5G networks will rely more on spectrum sharing than exclusive licenses. This is especially true for new higher candidate frequencies (> 6 GHz) that do not have a pre-existing spectrum regulation framework.

In the first part of the thesis, we tackle the challenge of providing higher data rates within limited spectral resources. Each SCN MNO has its own dedicated spectrum, and each MNO defines a percentage of how much its spectrum it is willing to share. The idea of the proposed CoPSS algorithms is that the spectrum is dynamically shared among MNOs based on their spectrum utilization, which is shared among MNOs in the network. This way interference can be avoided and spectrum utilization is maximized. Unused resources are shared equally between overloaded MNOs for a given time instant. Thus, only short-term fairness among overloaded SCNs can be guaranteed.

In the second part, we consider a multi-operator small cell network where MNOs share a common pool of radio resources. The goal is to ensure the long term fairness of spectrum sharing without coordination among small cell base stations. We develop a decentralized control mechanism for base stations using the Gibbs sampling based learning tool, which allocates suitable amount of the spectrum for each base station while avoiding interference from SCNs and maximizing the total network throughput.

In the studied scenarios, we show the importance of coordination among MNOs when the dedicated spectrum is shared. However, when MNOs share a common spectrum, a decentralized control mechanism can be used to allocate suitable amounts of spectrum for each base station. The proposed algorithms are shown to be effective for different network layouts, by achieving significant data rate enhancements with a low overhead.

Keywords: 5G, fairness in spectrum utilization, system level simulation

Luoto, Petri, Usean operaattorin välinen taajuuksien yhteiskäyttö piensoluverkoissa.
Oulun yliopiston tutkijakoulu; Oulun yliopisto, Tieto- ja sähkötekniikan tiedekunta; Centre for Wireless Communications; Infotech Oulu
Acta Univ. Oul. C 604, 2017
Oulun yliopisto, PL 8000, 90014 Oulun yliopisto

Tiivistelmä

Tämä väitöskirja keskittyy kehittämään uusia menetelmiä, joilla jaetaan taajuuksia useiden operaattoreiden kesken tulevista viidennen sukupolven verkoista alkaen. Päätavoite on parantaa tiedonsiirtonopeuksia sellaisissa piensoluverkoissa, joissa matkapuhelinoperaattorit jakavat joko heidän omia taajuusalueitaan tai heillä yhteisomistuksessa olevia taajuuksia. Kehitettyjen menetelmien suorituskykyä arvioidaan mittavien järjestelmätason simulointien avulla.

Matkapuhelinoperaattorit tyypillisesti omistavat yksin tietyt taajuusalueet, eivätkä ole valmiita jakamaan niitä. On kuitenkin oletettu, että tulevaisuudessa matkapuhelinoperaattorit joutuvat jakamaan taajuuksia, koska taajuusalueet ovat kalliita ja niukkoja erityisesti matalilla taajuusalueilla. Korkeammat taajuusalueet (> 6 GHz) puolestaan muodostavat otollisen alustan tehokkaalle spektrin jaetulle käytölle, koska niillä ei ole vielä olemassa olevaa taajuussääntelyä.

Väitöskirjan ensimmäisessä osassa keskitytään kasvattamaan tiedonsiirtonopeuksia kun jokainen matkapuhelinoperaattori omistaa oman taajuuskaistansa ja matkapuhelinoperaattorit määrittävät kuinka suuren prosentuaalisen osuuden ovat valmiita jakamaan. Esitettyjen algoritmien päätavoite on jakaa taajuuksia dynaamisesti matkapuhelinoperaattoreiden kesken. Algoritmeissa hyödynnetään tietoa matkapuhelinoperaattoreiden taajuuden käyttöasteesta, jonka matkapuhelinoperaattoritkommunikoivat toisilleen. Näin häiriö voidaan välttää ja taajuuden käyttö maksimoidaan. Käyttämättömät taajuudet jaetaan tasaisesti matkapuhelinoperaattorien kesken tietyllä ajanhetkellä. Näin voidaan taata lyhytaikainen oikeudenmukainen taajuuksien käyttö, mutta ei pitkäaikaista oikeudenmukaista taajuuksien käyttöä.

Väitöskirjan toisessa osassa matkapuhelinoperaattorit jakavat yhteisomistuksessa olevia taajuuksia. Tavoitteena on saavuttaa pitkäaikainen taajuuksien oikeudenmukainen käyttö, kun piensoluverkot eivät kommunikoi keskenään. Työssä kehitetään piensoluverkoille hajautettu algoritmi, joka perustuu oppimistyökaluun Gibbs-näytteistys. Näin saadaan allokoitua jokaiselle tukiasemalle tarvittava määrä taajuusresursseja niin, että häiriö tukiasemien välillä minimoidaan ja koko piensoluverkon suorituskyky maksimoidaan.

Tutkituissa skenaarioissa osoitetaan matkapuhelinoperaattoreiden välisen koordinaation tärkeys, kun jaetaan omia taajuusalueita. Toisaalta kun operaattorit jakavat yhteisomistuksessa olevia taajuuksia on mahdollista käyttää algoritmeja, joissa ei ole koordinaatiota matkapuhelinoperaattoreiden kesken. Väitöskirjassa vahvistetaan kehitettyjen algoritmien olevan tehokkaita ja sopivan monenlaisiin verkkoympäristöihin saavuttaen merkittäviä parannuksia tiedonsiirtonopeuteen ilman suuria kustannuksia.

Asiasanat: 5G, järjestelmätason simulaatio, oikeudenmukainen taajuuksien käyttö

To my family

Preface

The results of research in this thesis have been carried out at CWC Radio Technologies Research Unit, University of Oulu, Finland, during the years 2011-2016. I would like to give my many thanks to all the people in the CWC who have inspired me a lot.

First and foremost, I would like to express my deepest gratitude to my supervisor Prof. Matti Latva-aho. He provided me with the opportunity to do my PhD degree at the Centre for Wireless Communications. Without his continuous support, guidance and encouragement, my PhD thesis could not have been completed.

My special thanks also go to Dr. Pekka Pirinen for being a great advisor on research. His guidance helped me throughout the research and writing of this thesis. Additionally, my gratitude is extended to Dr. Mehdi Bennis who has also been a great advisor. Kari Horneman and Ling Yu from Nokia earn special thanks for suggesting this research direction and for giving invaluable feedback.

I would also like to thank my follow-up group, Prof. Jari Iinatti, Dr. Janne Janhunen and PhD. Muhammet Fatih Bayramoglu for their insightful advice and discussions during my doctoral program. I also extend my thanks to the pre-examiners, Prof. Klaus Moessner and Dr. Emilio Calvanese Strinati.

I am also very grateful to the whole administrative staff from the Department, specifically Hanna Saarela, Jari Sillanpää, Kirsi Ojutkangas, Eija Pajunen and many others. Furthermore, my thanks go to Infotech Graduate School for financial support of this thesis.

While conducting the research, I have been able to work on several projects, namely, Local Connectivity and Cross-Layer Design for Future Broadband Mobile Systems (LOCON), Solutions for Capacity Crunch in Wireless Access with Flexible Architectures (CRUCIAL), 5G radio access solutions to 10 GHz and beyond frequency bands (5Gto10G). The main funders of the projects were the Finnish Funding Agency for Technology and Innovation (TEKES), Nokia, Huawei Technologies, Anite Telecoms/Keysight Technologies, Broadcom Communications Finland, Elektrobit Wireless Communications and Infotech Oulu Graduate School. I have also received personal funding from the Nokia Foundation, Finnish Foundation for Technology Promotion, Riitta and Jorma J. Takanen Foundation, Walther Ahlström Foundation, Ulla Tuominen Foundation, and Tauno Tönning Foundation. All these funders are highly appreciated.

I am grateful to my parents, Aila and Martti, for their support and encouragement towards my education. I am also grateful for my siblings Jaana, Outi, Maarit, and Markus. Finally, I would like to express my deepest gratitude to my wife Piia, for always being by my side, loving, and supporting, and believing in me.

Oulu, January 2017 Petri Luoto

Abbreviations

1G	first generation
2G	second generation
3G	third generation
3GPP	3rd generation partnership project
4G	fourth generation
5G	fifth generation
ACK	acknowledgement message
ASA	authorized shared access
BG	Boltzman-Gibbs
CBRS	citizens broadband radio service
CC	component carrier
CDF	cumulative distribution function
CoPSS	co-primary spectrum sharing
CQI	channel-quality indicator
D2D	device-to-device
DAS	distributed antenna system
ETSI	European Telecommunications Standards Institute
EU	European Union
FCC	Federal Communications Commission
EVM	error vector magnitude
FDD	frequency division duplex
FEP	frame error probability
FER	frame error rate
GSCM	geometry-based stochastic channel model
HARQ	hybrid automatic repeat request
HSPA	High Speed Packet Access
ISM	industrial, scientific, and medical
ITU-R	International Telecommunication Union Radiocommunications
LSA	licensed shared access
LTE	Long Term Evolution

LTE-A	Long Term Evolution Advanced
L2S	link-to-system
MCS	modulation and coding scheme
METIS	Mobile and wireless communications Enablers for Twenty-twenty
MIESM	mutual information effective SINR mapping
MIMO	multiple-input and multiple-output
MNO	mobile network operator
MRC	maximum ratio combining
MTC	machine-type communication
NACK	negative acknowledgement message
NLOS	non-line-of-sight
NRA	National Regulatory Authority
OFDM	orthogonal frequency-division multiplexing
OFDMA	orthogonal frequency-division multiple access
PF	proportional fair
PL	path loss
PMF	probability mass function
PRB	physical resource block
QoS	quality of service
RRH	remote radio heads
SAPHYRE	Sharing Physical Resources Mechanisms and Implementations for Wireless Networks
SAS	spectrum access system
SCN	small cell network
SDN	software defined networking
SINR	signal to interference and noise ratio
SU	spectrum utilization
UDN	ultra-dense network
UE	user equipment
WSR	weighted sum rate

$\mathbf{A}$	adjacency matrix of SCN
$\hat{\mathbf{A}}$	adjacency matrix of overloaded SCN
A_{in}	penetration loss of internal wall
$\mathscr{A}_b$	action space of SCN b

$\mathscr{B}$	a set of SCNs
B_v	v number of vertices (SCNs) in the graph
b	SCN
b^+	all the overloaded SCNs
$E(\cdot)$	mathematical expectation
E_v	v edges in the graph
$\overline{f(t)}$	time average cost function
G_v	v number of graphs
G_b	Boltzmann-Gibbs distribution
J	Jain's index
K	users connected to SCN b
k	number of penetrated walls
$\mathscr{L}$	a set of MNOs
$\hat{\mathscr{L}}_i$	a set of MNOs, which are overloaded neighbors
$\check{\mathscr{L}}_i$	a set of MNOs, which are not overloaded neighbors
$\mathscr{N}(b_i)$	a set of not neighboring vertices of b_i
N_{c}	number of subcarriers
N_{r}	number of receiver antennas
N_{t}	number of transmit antennas
N_{cc}	number of CCs
$\mathscr{N}_{\mathrm{nol}}$	a set of not overloaded neighbors
$\mathscr{N}_{\mathrm{ol}}$	a set of overloaded neighbors
$\hat{n}$	co-located overloaded SCNs
Q	number of PRBs
$\mathbb{R}$	real number field
$R_b^{\mathrm{cc}}(\tau)$	summation of the bits that can be transmitted over all the CCs in the common pool
$R_b^{\mathrm{D}}(\tau)$	achievable rate of SCN b when the dedicated spectrum is used
R_b^{T}	users sum rate target when served by SCN b
S	sharing factor
T	time window
u_b	utility at SCN b
$\hat{u_b}$	averages of utility estimation
$\mathscr{V}$	configuration space
$\bar{v}_b(t)$	moving time average of the spectrum usage over time window T

v_0	central controller
$v_{\max}$	pre-agreed maximum spectrum sharing ratio among operators
W_l	number of free PRBs from MNO l
x_b	a suitable set of CCs for SCN b
$\tilde{x_b}$	estimated number of CCs needed
α	regularization coefficient of the spectrum violation
γ_b	learning rate for utility function
ε	learning rate for mixed strategy probability distribution
κ_b	temperature
π	mixed strategy probability distribution
$\pi(0)$	initialization distribution
$\tilde{\pi}$	modified initial distribution

Contents

1 Introduction

1.1 Motivation

Fifth generation (5G) mobile communication systems are expected to revolutionize everything seen so far in wireless systems [1–4]. 5G requirements depend on the targeted application but will include data rates ranging from very low sensor data to very high video content delivery, ultra-reliable and low latency communication, low energy consumption, and high reliability. These technological requirements are expected to be achieved while maintaining a similar or lower cost than today's technologies.

Cellular networks were originally designed for providing voice only services [5–8]. However, cellular standards are in constant evolution and each of the cellular standards has evolved around a set of key use cases. The first generation (1G) was dedicated to voice services. In the second generation (2G) the objective was to improved voice and text messaging. In the third generation (3G) the main goal was to integrate voice and affordable mobile Internet together. Finally, in the fourth generation (4G) the design target was to provide high capacity mobile multimedia services. 5G networks are expected to be available in 2020. The existing technologies will evolve side by side with new technologies. Thus, technologies such as High Speed Packet Access (HSPA) and Long Term Evolution-Advanced (LTE-A) will continue to evolve and will provide the backbone of the overall radio access solution.

5G is likely to integrate enhancements in legacy radio access technologies with new developments in the areas of multiple access, waveform design, interference management, access protocols, network architecture and virtualization, massive multiple-input and multiple-output (MIMO), full-duplex radio technology, low latency, device-to-device (D2D) and machine type communication (MTC) and mission-critical applications, etc. [4, 9].

In addition to advances in radio access technology, network capacity and connectivity can be improved by network densification, mainly via small cell networks (SCNs) and by harnessing broader spectrum allocations. In addition to SCN deployments, there are many other techniques and systems that can improve coverage and data rates in densely populated indoor environments. These techniques include the deployment of remote radio heads (RRHs), distributed antenna systems (DAS), Wi-Fi access points, etc. The use of LTE SCNs offers several advantages over such systems. Compared with

DAS, LTE SCNs are both cheaper and less complex to deploy [10], and compared to Wi-Fi, LTE SCNs offer better performance, more efficient use of resources, and are well designed to support a substantial number of users [11].

SCNs are interesting to network operators because it is estimated that 2/3 of the calls and over 90 percent of data services occur indoors and some surveys show that between 30-45 percent of users experience poor indoor coverage [10]. Furthermore, it is expected that 78% of traffic will go through small cells by 2020 [12]. When SCNs are deployed inside homes or in public indoor places, e.g., in the shopping mall, users will have high quality and high data rate services indoors. Moreover, SCN removes the need to deliver indoor services from macrocells, which is not efficient.

Future networks are expected to include innovative ways of sharing both spectrum and hardware [13]. This can be seen by observing current trends [14]. In current wireless communication networks, mobile network operators (MNOs) have commonly acquired exclusive usage rights for certain frequency bands and have little incentive to share them with other operators, despite significant research and regulatory efforts. This might be due to the lack of joint technological and business consideration. However, due to high cost and spectrum scarcity at lower frequencies it can be expected that efficient use of the spectrum in 5G networks will rely on spectrum sharing rather than exclusive licenses.

When SCN and spectrum sharing techniques are merged the potential of small cells becomes even higher. In the future, small cells with spectrum sharing will be one of the key features in smart homes, where all the devices (phones, tablets, sensors, etc.) can be connected to their closest small cell. For this purpose, in this thesis we different aspects of spectrum sharing with an indoor multi-operator SCN. The main focus is on analyzing methods for co-primary sharing (CoPSS), which is a recently proposed novel spectrum sharing mechanism geared towards 5G systems [15].

1.2 Literature review

This section reviews the main components related to spectrum sharing. Specifically, different spectrum access modes and resource allocation are shortly described. Then, general multi-operator spectrum sharing approaches are reviewed. Moreover, the selected CoPSS sharing method is reviewed in detail.

1.2.1 Spectrum access modes and radio resource management

The future spectrum landscape for mobile communication systems is complex and different bands will be made available under different regulatory approaches [16]. Furthermore, from different regulatory scenarios a set of spectrum usage scenarios can be derived as shown in Fig. 1. The classification follows spectrum access modes and sharing scenarios proposed in [15]. Multiple frequency bands, subject to different regulation including various forms of shared spectrum, are expected to be available. Some frequency bands are already assigned for 5G networks, the Federal Communications Commission (FCC) has approved spectrum for 5G including carrier frequencies at 28 GHz, 37 GHz and 39 GHz [17]. The spectrum is at higher carrier frequencies than currently used.

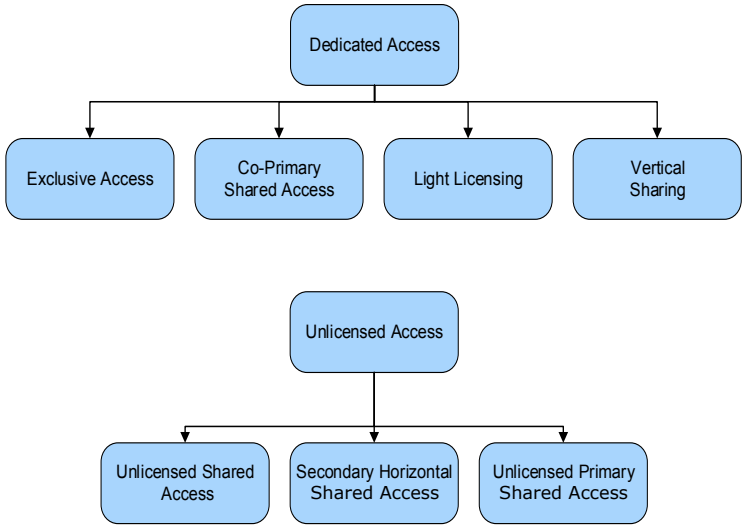

Fig. 1. Spectrum access and authorization. [15]

From a radio resource management point of view, a vast number of different resource allocation methods have been proposed in the literature for different spectrum access modes. Based on the information exchange between base stations, resource allocation methods can be divided into centralized, clustered and distributed methods. The coordination between MNOs should be minimal because MNOs may not want to share operator-specific information with their competitors [18]. Thus, information exchange among MNOs is a critical design factor for spectrum sharing algorithms.

In *dedicated access* the usage rights of the spectrum are exclusive to time, frequency and geographic region. Licenses are granted by the National Regulatory Authority (NRA) usually through an auction for MNOs [19, 20]. Under dedicated access, the following access schemes can be defined: *exclusive access*, *co-primary shared access*, *light licensing*, and *vertical sharing*.

Exclusive access

In exclusive access, the system does not have to share the communication resources with any other system or service of equal or higher priority. The license owner can utilize the spectrum according to the assignment rules either nation-wide or just within a certain region or locally. For example, cellular networks and broadcasting fall under exclusive access.

When MNOs operate on their own exclusive spectrums, base stations allocate the spectrum and coordinate the interference management (intra-cell and inter-cell) together with user equipment, which provides channel state information back to the base station. The idea of inter-cell interference coordination (ICIC) is to avoid the worst-case interference situations between base stations operated by the same MNO [21]. ICIC techniques can be classified into mitigation and avoidance techniques [22]. Interference can be mitigated using interference cancelation [23], for example or adaptive beamforming [24]. In interference avoidance techniques the idea is to minimize or avoid the interference as much as possible [25–27]. Interference can be avoided in time or frequency domain or by controlling power levels. However, different ICIC methods would require fast/real-time information exchange among base stations of different MNOs so they are not feasible methods for spectrum sharing [28].

Co-primary shared access

In co-primary shared access, the primary license holder agrees on the joint use of their spectrum or part of it. The idea is that there are mutual agreements between MNOs on how the spectrum is shared and what the rules are. MNOs can share their dedicated spectrums (spectrum pooling) or MNOs can jointly own the common spectrum pool (mutual renting). Even though MNOs have mutual agreements on how to share the spectrum, the operator specific information that is shared among different MNOs should be minimal. Therefore, software defined networking (SDN) and game theoretical

approaches are proposed for allocating resources in co-primary shared access scenarios [29–31]. Co-primary shared access methods are analyzed in detail in Section 1.2.3.

Light licensing

Light licensing is an approach where a procedure for issuing a license is simplified compared to traditional licensing [32]. The additional users are authorized to use the spectrum (or part of the spectrum) in accordance with sharing rules included in their spectrum usage rights. In this case, a certain quality of service (QoS) can be guaranteed to all the authorized users. Furthermore, it is expected that light licensing is used in frequency bands where the risk of interference is low. Promising frequency bands for light licensing are around 60 GHz and 80 GHz [28].

Vertical sharing

Under vertical sharing three different sharing schemes can be defined: *licensed shared access (LSA), authorized shared access (ASA), and spectrum access system (SAS)* [33, 34]. ASA/LSA is a regulatory concept that allows license holders (incumbents) to share a spectrum with other service providers under well-defined conditions [14]. The idea is that an MNO can access the underutilized spectrum on a shared basis without interfering with incumbent spectrum holders. The utilization of the spectrum is very low in time and/or location. The best use case for ASA is for small cells where they can be deployed geographically closer to incumbent spectrum users due to their lower transmitting power. Existing mobile technology and 3rd Generation Partnership Project (3GPP) standards allow cost-effective deployment using the available LTE infrastructure.

The SAS concept is very close to the LSA concept. In the SAS concept, three hierarchical tiers can be identified [35]. The first tier, similarly to the LSA framework, is the primary or incumbent user. The second tier is a commercial service provider, for example an MNO. In the third tier, the tertiary users operate, e.g., very lightly licensed users. The tertiary users can access the spectrum when neither the primary nor the secondary users are present. The FCC has proposed a citizens' broadband radio service (CBRS) on a 3.5 GHz band, which is a three-tiered spectrum authorization framework to accommodate a variety of commercial uses on a shared basis with incumbent federal and non-federal users of the band [36]. In [37–39] the performance of a heterogenous network coexisting with the radar system at 3.5 GHz is evaluated. Furthermore, in [40] a

spectrum sharing algorithm is proposed to allocate resources between a cellular network and a radar system.

Unlicensed access

In *unlicensed access*, rights are generally granted without an individual license but subject to certain technical restrictions or conditions, e.g., limited transmitting power [28]. Usually, the spectrum is shared between a large number of users who have very different requirements and different use cases. System performance is difficult to predict, but the spectrum cost is low, because the cost for an unlicensed spectrum is typically zero. Under unlicensed access the following access schemes can be defined: *unlicensed shared access*, *secondary horizontal shared access*, and *unlicensed primary shared access.* In unlicensed shared access allocated frequencies can be utilized by several users. No primary service is allocated to these bands and there are no protection rights. The best example of this is the industrial, scientific, and medical (ISM) radio band. Secondary horizontal shared access is close to the unlicensed shared access scheme but secondary users are obligated to protect the higher priority spectrum users. Finally, in unlicensed primary shared access a primary service is allocated in a frequency band and all the services using the same technology can use this frequency band. Multiple technologies are used in unlicensed spectrum such as Wi-Fi, LTE in unlicensed and Bluetooth. The main challenge is the unpredictable QoS. An unlicensed spectrum is most suitable for local area access, and opportunistic mobile broadband usage.

1.2.2 Multi-operator spectrum sharing approaches

The International Telecommunication Union Radiocommunications (ITU-R) has been looking into using licensed white spaces [41]. The European Telecommunications Standards Institute (ETSI) on the other hand has been focusing on spectrum sharing by applying radio environment maps (REMs) [42, 43]. The 3GPP has considered spectrum sharing in LTE networks [44, 45]. Many different aspects of spectrum sharing have been considered in EU projects such as Mobile and wireless communications Enablers for Twenty-twenty (2020) Information Society (METIS) [9] and Sharing Physical Resources Mechanisms and Implementations for Wireless Networks (SAPHYRE) [46].

Already two decades ago a comprehensive survey was done in [47] for dynamic channel assignment for various cellular and non-cellular applications. More recently,

multiple spectrum sharing surveys have been conducted in [48–53]. In these surveys the following concepts have been studied: cognitive radio networks, as well as opportunistic and dynamic spectrum access. The most recent survey [28] provides a comprehensive overview of licensed spectrum sharing mechanisms for cellular systems. The paper focuses on dynamic spectrum sharing, different sharing scenarios, and evaluating the major challenges of spectrum sharing.

Multi-operator spectrum sharing has been considered in many studies over the years in the literature, e.g., in [54–58]. These papers investigated such concepts as dynamic spectrum allocation and spectrum refarming, which support different generations of cellular networks operating in the same radio spectrum. In [59], the problem of spectrum sharing in a cellular radio network is recognized both from the perspectives of economics and network performance. Greedy and Round Robin scheduling were proposed to redistribute call loads between base stations and facilitate sharing of the spectrum. The protocols proved to be simple yet effective. Furthermore, in [60] it is shown that sharing different resources in a network provides an increase in overall spectral efficiency, in the presence of variable data rates.

Simple distributed algorithms are proposed in [61] to dynamically redistribute the available frequency resources among femtocells based on local interference measurements when operators agree on the sharing of their spectrum bands. The proposed algorithm improves performance. Furthermore, it is shown that spectrum sharing among operators is advantageous to ensure QoS to their subscribers. Various aspects of inter-operator resource sharing, such as analyzing efficient coordination mechanisms and developing frameworks for infrastructure sharing, are studied in [46]. Furthermore, new self-organizing physical layer resource sharing models are developed. In [62], the potential gain of spectrum sharing between cellular operators is investigated in terms of network efficiency. Moreover, different network topologies and parameters are closely related to the achievable gains that are in the range between 10 and 100 percent. Moreover, in [63], inter-operator sharing of cellular resources including capacity, spectrum and base stations is investigated. Results indicated that inter-operator sharing options were effective only when there were large differences in resource utilization between the two networks.

The main target of each study has been to improve spectral efficiency while trying to guarantee some level of fairness among MNOs. It can be concluded that current cellular standards and base station hardware may support and benefit from spectrum sharing.

However, most of the multi-operator spectrum sharing research has been done in macro cell networks.

1.2.3 Co-primary spectrum sharing studies

One of the advanced spectrum sharing techniques is co-primary spectrum sharing (CoPSS), which is proposed as a sharing mechanism for 5G systems, where any MNO is allowed to utilize the shared spectrum allocated for 5G cellular systems. In [15], CoPSS is defined as a spectrum access model where primary license holders agree on the joint use of (or parts of) their licensed spectrum. This would be possible in the small cell domain only where base station coverage is similar to today's Wi-Fi access points and the frequency band is dedicated to small cell use.

In [29] CoPSS together with SDN architecture is proposed. Required roles for both architectures and information exchange between the corresponding entities are identified in order to enable spectrum trading. Furthermore, it is highlighted that the proposed architecture could be applied in other sharing schemes such as LSA. A similar SDN architecture to CoPSS is also considered in [30]. Therein, a soft inter-operator interference coordination mechanism is proposed for CoPSS in an ultra-dense network (UDN). It is shown that the proposed mechanism can improve the network spectrum and energy efficiency vastly when compared to the no sharing scenario. In order to guarantee the fairness for MNOs the importance of the agreement with some parameters is noted. However, in the proposed method no sensitive information exchange among MNOs is required, which is more attractive in terms of practical implementation. In [64] and [65] CoPSS is studied in the MIMO multiuser scenario where two small cells were deployed in the downlink transmission. Resource allocation with a joint precoder and decoder design is proposed for weighted sum rate (WSR) maximization problem. The problem is non-convex and therefore the main problem is separated into two sub-problems. In the first subp-roblem, subcarriers are allocated to the users. In the second, a joint precoder-decoder design is employed after the static resource allocations are acquired from the first sub-problem.

A CoPSS method for multiple MNOs in dense local area deployment is considered in [66]. A realistic system framework is formulated to guarantee reliable and efficient communications within a denser network. The proposed solution is easy to control and incurs low signaling overhead, which can be implemented in practical systems. It is

shown that the proposed method is beneficial for the system performances in terms of the system throughput, and cell edge throughput.

In [18], CoPSS protocol is proposed in an indoor deployment scenario with frequent network load variations that are expected for small cell deployments. The proposed protocol is distributed and does not require operator-specific information exchange, and incurs a minimal communication overhead between the MNOs. The protocol is based on a book keeping of spectrum usage favors asked and received by the MNOs. Thus, long term fairness can be guaranteed and MNOs can enhance their QoS in comparison to a scheme where no spectrum sharing is allowed. Moreover, this work is extended in [67], in which two small cell operators are deployed in the same geographical area. MNOs share spectrum resources from a common pool. A method is investigated to coordinate the utilization of the spectrum pool without monetary transactions and without revealing operator-specific information to other parties. Each MNO has equal access rights to a spectrum pool. Spectrum sharing is modelled as a non-cooperative repeated game where an MNO may ask for spectrum usage favors from its competitors. A spectrum usage favor means that the competitor would stop using some component carriers from the pool. The proposed strategy is shown to be better when compared to the case without coordination between the MNOs.

In [68], a CoPSS scenario where operators have similar rights for accessing spectrum is evaluated. A coordination protocol assuming an agreement to a set of negotiation rules was designed. The signaling overhead is low and other MNOs' channel state information is assumed to be unknown. The results show that two MNOs are both able to offer higher user rates than they could without coordination. Furthermore, when an MNO knows that other MNOs have networks with similar characteristics and everyone is rational, there is some incentive to coordinate spectrum usage. In [31], a multi-operator CoPSS scenario for D2D setting is tackled. Interactions are modelled as a non-cooperative game. The idea is that MNOs offer some amount of spectrum to contribute to multi-operator D2D communication considering only its individual performance while taking into account the offer made by the opponent operator.

An adaptive CoPSS shared access scheme is proposed in [69]. The spectrum is adaptively partitioned into private and non-orthogonally shared parts. A significant gain is obtained when the proposed scheme is used, especially in the case of high and moderate external interference. In [70], CoPSS is modelled as a one-shot game. Each MNO proposes a spectrum partition that maximizes its own sum utility, and the actual spectrum partition is resolved based on a priori decision rules that reflect the regulatory

framework. Thus, the signaling information is minimal among MNOs. Simulation results show that adaptive spectrum sharing is able to outperform the baseline model.

One important aspect of spectrum sharing is the business aspect for MNOs [28]. The deployment of spectrum sharing introduces economic and business concerns to the stakeholders. Spectrum sharing can create new additional costs, e.g., additional infrastructure may be required. Acquiring licenses together with multiple MNOs is more cost efficient but the challenge is how to guarantee access and how the cost is divided among MNOs. Different solutions are proposed for this scenario such as bidding or leasing [71–76]. In [77] and [78] the business aspects for CoPSS are analyzed and the key points are identified. The current spectrum scarcity and new business potential, especially in hotspots and small cells, are seen as enabling factors for CoPSS. The key idea of CoPSS is that a licensed spectrum is shared among competing MNOs according predefined policies and rules. A shared license may include the dedicated share for the base operation for each MNO and other stakeholders. Furthermore, it is possible to utilize LTE ecosystem for all services to ease the standardization efforts. Finally, it is concluded that CoPSS is a potential candidate for MNO business operations in the near future. More information about the business aspects can be found in [79–83].

The main difference in each CoPSS study compared to general multi-operator spectrum sharing approaches is that CoPSS papers focus mainly on spectrum sharing among small cell MNOs, which is the best scenario for CoPSS. In this thesis, similar scenarios and design goals are tackled. The target is to develop low overhead algorithms in a realistic small cell network scenario, while MNOs share a minimal amount of operator-specific information or no information exchange at all. Furthermore, we show the benefits from using higher frequencies due to network densification, while mobile network operators share a common spectrum.

5G spectrum management has to be flexible enough to support many advanced spectrum sharing techniques. For this thesis, we have selected CoPSS as the sharing method, because it is a promising sharing method already for the existing LTE ecosystem and for 5G networks. Spectrum access in the CoPSS is further divided into two cases: dedicated spectrum sharing (spectrum pooling), and common spectrum sharing (mutual renting).

1.3 Objectives, contributions, and outline of the thesis

The objective of this thesis is to analyze and optimize multi-operator small cell networks. The idea is to use self-organizing network (SON) techniques to solve interference problems with shared radio resources and find efficient techniques for spectrum sharing between operators [84]. SON aims to automate the configuration of mobile networks and to cut operational expenditure while improving network quality.

There are different ways the spectrum sharing could be done. The first scenario is that operators would be willing to share some percentage of their own band if it is unused. The second scenario is that there would exist an extra common band that operators own jointly. This type of spectrum sharing creates an interesting resource allocation and management problem. Also, the interference environment is challenging, e.g., what happens if the other operator starts using resources which are already utilized by another operator even though shared resources should be unused. The main target is to maximize the total network throughput while guaranteeing long and short term fairness among operators.

The aforementioned problem is fundamental in future 5G networks because it is expected that the efficient use of the spectrum in 5G networks will rely on spectrum sharing rather than exclusive licenses. Cognitive radio solutions for multi-operator radio access networks can be used to solve resource allocation and interference challenges. Centralized control for multi-operator spectrum sharing requires coordination among MNOs, which introduces extra signaling. Therefore, distributed solutions are needed. In this thesis answers to the following questions are sought: What type of signaling is needed between operators? How often should base stations/operators share information? What and how accurate should this information be? Would information be shared between operators or through a central controller? What type of spectrum sharing is the most efficient: a common shared spectrum, or partial or full spectrum sharing? How can you ensure fairness between operators? How much gain can we achieve?

This thesis focuses on the development and analysis of different CoPSS algorithms. The thesis is divided in two parts: in the first part, each SCN MNO has its own dedicated spectrum, and each MNO can define a percentage of how much spectrum it is willing to share. In the latter part of the thesis, MNOs share a common pool of radio resources. Moreover, the goal is to ensure the long-term fairness of spectrum sharing without coordination among small cell base stations. The following is the detailed outline of the thesis:

– **Chapter 2**: We present some relevant theoretical tools suited well to evaluating CoPSS algorithms, namely graph theory and machine learning. Both methods are particularly useful for studying network management related issues such as resource allocation and interference management. Graph theory related models are utilized in Chapter 3 and a learning-based tool is used in Chapter 4.
– **Chapter 3**: We consider a scenario where each SCN MNO has its own dedicated spectrum, and each MNO can define a percentage of how much spectrum it is willing to share. An MNO enables spectrum sharing when an SCN is not using 100% of its spectrum. A given SCN is not fully utilizing its spectrum when it can provide the required data rate for all the users without using 100% of its spectrum. Furthermore, the spectrum is dynamically shared among MNOs based on their spectrum utilization, which is shared among MNOs in the network. This way interference can be avoided and spectrum utilization is maximized. Unused resources are shared equally between overloaded MNOs for a given time instant and only short-term fairness among overloaded SCNs can be guaranteed. We propose three centralized algorithms and one decentralized algorithm for CoPSS. The proposed algorithms use a moderate amount of shared information among MNOs/SCNs and they do not require long iterative information exchange processes. Thus, the proposed CoPSS algorithms are practical.
– **Chapter 4**: We investigate a scenario where MNOs share a common pool of radio resources, in which the goal is to ensure long term fairness of spectrum sharing without coordination between small cell base stations. We develop a decentralized control mechanism for base stations using the Gibbs sampling based learning tool, which allocates a suitable amount of the spectrum for each base station. We propose three decentralized algorithms (Gibbs, Gibbs+penalty and Gibbs+distribution) for CoPSS and compare them with three state-of-art algorithms (No sharing, Greedy and Equal). The proposed decentralized algorithms do not require sharing any information between MNOs/SCNs. Thus, the proposed CoPSS algorithms are suitable for practical implementations.
– **Chapter 5**: Finally, conclusions and discussion about open problems for future research directions are given.

1.4 Author's contribution to the publications

The thesis is written as a monograph based on two journal papers [85] and [86] and two conference papers [87] and [88]. In [85], CoPSS algorithms are developed and

analyzed when MNOs share their dedicated spectrum. In [87] CoPSS algorithms are developed and analyzed when MNOs share a common spectrum pool. This work is extended in [86] where a new algorithm is introduced and an analytical study is conducted. In [88] the main goal is to show the benefits of using higher frequencies due to network densification, while mobile network operators share a common spectrum. The author of this thesis had the main responsibility for developing the original ideas, deriving the algorithms, implementing the algorithms on a system level simulator based on MATLAB, generating the numerical results, and writing the papers. The role of other co-authors was to provide guidance, support and comments on developing the ideas/algorithms as well as writing the papers.

2 Resource allocation and coordination

This chapter reviews the main tools that are used in this thesis to solve the spectrum allocations in the small cell networks. Resources in the network can be allocated either in a centralized, decentralized or distributed manner. Fig. 2 illustrates the difference between these network topologies. When resources are allocated in centralized manner a central controller is required. A clustered network consists of a network of multiple centers, whereas in a distributed network a base station can make a decision alone based on information exchange between nodes in the network. In this thesis these different approaches are analyzed by utilizing graph theory and learning based tools for allocating the spectrum in small cell networks (SCNs).

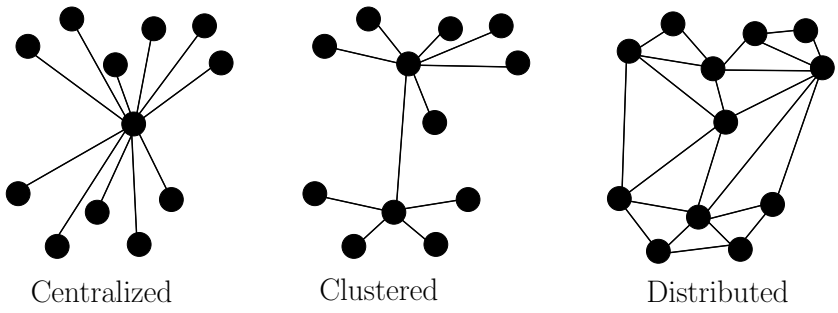

Fig. 2. Graph presentation of centralized, clustered and distributed network.

2.1 Graph theory

Graph theory originates from the 1736 Leonard Euler's paper "The Seven Bridges of Königsberg", where the question was whether a person could plan a walk in such a way that he would cross each of the bridges once but not more than once [89]. This paper was a foundation for graph theory. During the 20th century graph theory developed into a substantial body of knowledge. Graph theory is utilized in many different fields such as physical, biological, and information studies, since many practical problems can be modeled as a graph.

Graph theory has been extensively applied in wireless communication, where it is used to solve resource allocation problems. In [90] the target is to mitigate cross-tier and co-tier interference in a dense SCN. A centralized dynamic radio resource allocation

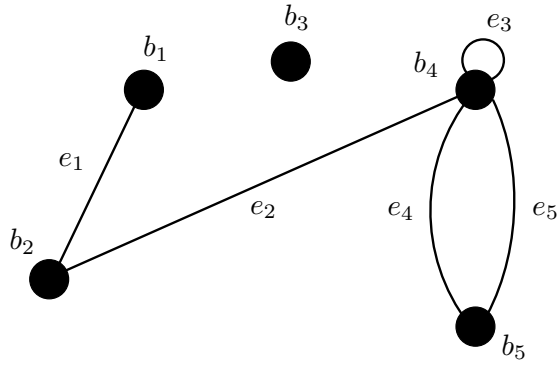

Fig. 3. Graph with vertices and edges.

method exploiting graph theory approach is proposed. When a centralized approach is used it can cause a high amount of overhead due to signaling to the controller. This problem is avoided by only coordinating if interference between nodes is high. Even though coordination is required, the achieved gain in throughput exceeds the extra overhead.

In [91] resources are allocated using cognitive radio technology and interference among nodes is avoided by graph coloring. The idea of graph coloring is to assign different colors for adjacent base stations. The proposed graph coloring algorithm improves the average SINRs and outperforms state-of-the-art algorithms. Furthermore, in [92] graph coloring is also utilized to improve the throughput of cell-edge users. In this work the central controller only needs the cell identification of the interfering neighbors and determines the sub-band assignment by using a graph coloring and search algorithm. The limitation is that the algorithm only works if there is only one user per base station. The authors of the previous work extend their work in [93]. The new algorithm utilizes both central and autonomous resource assignment approaches. Cell-edge and system capacity is further improved.

A graph is constructed from vertices and edges as shown in Fig. 3. Vertices are the connection points (e.g. base stations) in the graph and edges are the lines connecting edges (e.g. communication link between base stations). Let $G = (B,E)$ denote the graph, where $B = \{b_1,\ldots,b_5\}$ denotes the set of vertices and $E = \{(b_1,b_2),(b_2,b_4),(b_4,b_4),(b_4,b_5),(b_5,b_4)\}$ denotes the set of edges. In graph theory, the following terminology is used to define graphs [94]:

– Edges that have the same end vertices are parallel.

– A graph is simple if it has no parallel edges or loops.
– An empty graph has no edges.
– A null graph has no vertices.
– A graph with one vertex is trivial.
– Edges are adjacent if they share a common end vertex.
– The degree of the vertex defines the number of edges connected to the vertex.
– A graph is complete if all the vertices are connected to each other (simple graph)
– A complete subgraph of G is called a clique of G. Every two distinct vertices in the clique are adjacent.

The adjacency matrix of the graph $G = (B, E)$ is an $n \times n$ matrix $\mathbf{A} = (d_{ij})$, where n is the number of vertices in G and d_{ij} is the number of edges between b_i and b_j. When $d_{ij} = 0$ if (b_i, b_j) is not an edge in G. The adjacency matrix from the graph shown in Fig. 3 can be defined as follows:

$$\mathbf{A} = \begin{bmatrix} 0 & 1 & 0 & 0 & 0 \\ 1 & 0 & 0 & 1 & 0 \\ 0 & 0 & 0 & 0 & 0 \\ 0 & 1 & 0 & 1 & 2 \\ 0 & 0 & 0 & 2 & 0 \end{bmatrix}.$$

Graph coloring is one of the most well-known and studied aspects of graph theory. In the mid nineteenth century, the so called Four Color Problem was an inspiration for the development of graph coloring. In wireless networks, as mentioned earlier, the main idea of graph coloring is to assign different colors for adjacent base stations [95]. A different color will indicate that adjacent base stations are using different transmission frequencies, for example. The idea of vertex coloring for a given graph G is to color all the vertices of the graph with different colors. After the vertex coloring, any two adjacent vertices of G have different colors.

One way to identify adjacent base stations is to utilize clustering. By exploiting the knowledge on the location of each SCN, the central controller measures the similarity between SCNs based on the distances and groups them into multiple clusters. The similarity between two SCNs $b, b' \in \mathscr{B}$ with their locations y_b and y'_b is measured by the Gaussian similarity function as follows [96]:

$$s_{b,b'} = \exp\Big(\frac{-||y_b - y_{b'}||^2}{2\sigma^2}\Big), \tag{1}$$

where σ controls the impact of neighborhood size. The distance-based similarity matrix $\mathbf{S}$ is formed using $s_{b,b'}$ as the (b,b')-th entry. The idea behind (1) is that SCNs located far from each other have low similarities, and as they come closer, their similarities increase leading the SCNs to be more likely in the same cluster. Using the similarities $\mathbf{S}$ of the SCNs, spectral clustering can be determined[1]. The spectral clustering method exploits both the connectivity and the compactness of nodes in a graph, which is the geometry of the SCN distribution in the network. The number of clusters k is a vital input for spectral clustering. For a given neighborhood size, sparse networks consist of SCNs that are isolated from each other, and thus a large k is needed. For dense networks, most of the SCNs are close to each other, and thus a small k is sufficient. Therefore, an efficient choice of k for a given neighborhood size can be presented as follows [97]:

$$k = \arg\max_i(\zeta_{i+1} - \zeta_i), \quad i = 1, \ldots, |\mathscr{B}|, \tag{2}$$

where ζ_i is the i-th smallest eigenvalue of the network Laplacian matrix $\mathbf{L}$. Here, the network Laplacian matrix is formed at the central controller as $\mathbf{L} = \mathbf{D} - \mathbf{S}$, where $\mathbf{D}$ is the diagonal matrix with the b-th diagonal element as $\sum_{b'=1}^{|B|} s_{b,b'}$.

In this thesis, an adjacency matrix is used in order to generate interference free resource allocations between nodes in the network. It is assumed that the SCNs communicate with each other if the distance is less than or equal to 50 meters. When the SCN is further away, the interference caused to other SCN users is not significant anymore. This way the SCNs that are isolated can utilize the shared spectrum efficiently.

2.2 Gibbs sampling

In order to address the problem of spectrum sharing in a distributed manner, a reinforcement learning tool can be utilized for allocating resources autonomously [98]. The idea of reinforcement learning is to automatically learn how to allocate resources with little or no built-in system specific knowledge.

In [99] an algorithm based on reinforcement learning is proposed that allows each transmitter to learn both its optimal strategy and the values of its expected utility for all its actions. The main problem of the proposed algorithm is how to accelerate the convergence rate of the learning algorithms. However, the reinforcement learning tool is seen as a good option to further develop distributed control and radio resource allocation.

[1] For the interested readers, the details of spectral clustering can be found in [97].

This work is extended in [100] to provide an interference mitigation technique for cognitive femtocell networks.

In [101] a macro network with self-organizing network coordination is considered. The proposed algorithm is based on reinforcement learning and it is shown to improve the network stability. The work is extended in [102] for a heterogeneous network.

In this thesis, a reinforcement learning tool based on Gibbs sampling is used to solve spectrum allocations in SCNs. Gibbs sampling can be used to solve optimization problems for any node b in the following form

$$u_b = \max_{x \in \mathscr{A}} U_b(x) \tag{3}$$

where $U_b(x)$ is the utility function of node b and the variable x is a B-dimensional row vector with element x_b, $b = 1 \dots B$. Here, the feasible domain $\mathscr{A} = \prod_{b=1}^{B} \mathscr{A}_b$ is a compact set from the Cartesian product of the discrete sets $\mathscr{A}_b$ corresponding to x_b. The key idea of Gibbs sampling is that the value of each x_b is updated iteratively and asynchronously according to a probability distribution. Such a probability distribution can be captured by the Boltzmann-Gibbs (BG) distribution $G_b = (G_{b,1}, \dots, G_{b,|\mathscr{A}_b|})$, which is calculated as follows:

$$G_{b,i}\big(\hat{u}_b(t)\big) = \frac{\exp\big(\kappa_b \max(0, \hat{u}_{b,i}(t))\big)}{\sum_{\forall i' \in \mathscr{A}_b} \exp\big(\kappa_b \max(0, \hat{u}_{b,i'}(t))\big)}, \; i \in \mathscr{A}_b, \tag{4}$$

where $\kappa_b > 0$ is a temperature parameter that balances between exploration and exploitation and $\hat{u}_{b,i}(t)$ is the estimated utility of node b, which is the expected utility for each action over the time period $\{1, \dots, t-1\}$. For each time t, the joint utility and probability distribution estimations for any node b, $\hat{u}_b(t)$ and $\pi_b(t)$, are updated as follows;

$$\begin{cases} \hat{u}_{b,i}(t) & = \hat{u}_{b,i}(t-1) \\ & \quad + \gamma_b(t) \mathbb{1}_{\{x_{b,i} = x_b(t-1)\}} \Big(u_b(t) - \hat{u}_{b,i}(t-1) \Big), \\ \pi_{b,i}(t) & = \pi_{b,i}(t-1) \\ & \quad + \varepsilon_b(t) \Big(G_{b,i}\big(\hat{u}_b(t-1)\big) - \pi_{b,i}(t-1) \Big), \end{cases} \tag{5}$$

with the learning rates satisfying $\lim_{t\to\infty} \sum_{n=1}^{t} \xi(n) = \infty$ and $\lim_{t\to\infty} \sum_{n=1}^{t} \xi^2(n) < \infty$ for all $\xi = \{\gamma_b, \varepsilon_b\}$. A lower learning rate results a gradual learning (slow) process, which ensures a lower optimality gap (a gap between the current solution and the optimal solution). On the contrary, a higher learning rate provides an acute learning (fast)

process with a higher optimality gap [103]. By using the estimation $\hat{u}$, which needs to be calculated using a faster process, the optimal π can be found. Therefore, the relation between learning rates is such that $\lim_{t\to\infty} \frac{\gamma_b(t)}{\varepsilon_b(t)} = 0$. Our choices of learning rates are $\gamma_b(t) = t^{-\gamma}$ and $\varepsilon_b(t) = t^{-\varepsilon}$, with $0.5 < \gamma < \varepsilon < 1$. Here, $x_{b,i} = \frac{i-1}{N_{cc}}$ and the operator $\mathbb{1}_{\{x_{b,i}=x_b(t-1)\}}$ returns 1 if $x_{b,i} = x_b(t-1)$ is satisfied and 0 otherwise. The optimal solution can be obtained by Algorithm 2.1.

Algorithm 2.1 Gibbs sampling algorithm

1: Each node b initializes probability distribution $\pi_b(t-1) = [\pi_{b,i}(t)]_{i\in\mathscr{A}_b}$ and initial utility estimations $\hat{u}_b(t-1) = [\hat{u}_{b,i}(t)]_{i\in\mathscr{A}_b}$.
2: **while** $t > 0$ **do**
3: Each node b selects its action $x_b(t)$ based on its mixed strategy probability $\pi_b(t-1)$.
4: Calculate objective function $U_b(x)$
5: Update utility estimation and mixed strategy probability using (5).
6: $t \to t+1$
7: **end while**

2.2.1 Convergence and optimality discussion

Next, we prove that the system of coupled equations in (5) is a Gibbs field with steady-state distribution by invoking the Gibbs-Markov equivalence [104].

Theorem 1. Let $\boldsymbol{a}(t) = (a_1(t), \ldots, a_{|\mathscr{B}|}(t)) \in \mathscr{A}$ be the vector of actions played by all of the nodes following their mixed strategy probabilities, where $\mathscr{A} = \mathscr{A}_1 \times \cdots \times \mathscr{A}_{|\mathscr{B}|}$. Let $\boldsymbol{\pi}(t) = (\pi_1(t), \ldots, \pi_{|\mathscr{A}|}(t))$ with $\pi_i(t) = \Pr(\boldsymbol{a}(t) = \boldsymbol{a}_i)$ be the probability of selecting the ith action $\boldsymbol{a}_i \in \mathscr{A}$. Under Algorithm 2.1, as $t \to \infty$, $\boldsymbol{\pi}(t)$ converges to a stationary distribution $\boldsymbol{\Pi} = (\Pi_{\boldsymbol{a}}, \boldsymbol{a}\forall \in \mathscr{A})$ with,

$$\Pi_{\boldsymbol{a}} = \frac{\exp(\kappa \hat{u}_{\boldsymbol{a}})}{\sum_{\forall \boldsymbol{a}' \in \mathscr{A}} \exp(\kappa \hat{u}_{\boldsymbol{a}'})} \tag{6}$$

where $\hat{u}_{\boldsymbol{a}}$ is the ensemble average of the action $\boldsymbol{a}$'s utility estimation as $t \to \infty$.

Proof. Let u_b and $u = \sum_{\forall b\in\mathscr{B}} u_b$ be the ensemble averages of the utilities of node b and the network, respectively. As $t \to \infty$, for node b, the ensemble averages of utility estimation, and mixed-strategy probability become $\hat{u_b}$ and $\Pi_{b,i} = G_{b,i}(\hat{u_b})$ for $i \in \mathscr{A}_b$

as per (5), respectively. Since $\sum_{b\in\mathscr{B}} \hat{u}_{b,a_b} = \sum_{b\in\mathscr{B}} \hat{u}_b - u_b = \hat{u}_{\boldsymbol{a}} - u = \hat{u}_{\boldsymbol{a}}$ for any action $\boldsymbol{a} \in \mathscr{A}$, $\hat{\boldsymbol{u}} = (\hat{u}_{\boldsymbol{a}}, \forall \boldsymbol{a} \in \mathscr{A})$ is the ensemble average of the utility estimations for the entire system. Since an action $\boldsymbol{a}$ of the system is composed by the set of actions $(a_{b,i_b}, \forall b \in \mathscr{B})$ per each node, the probability of selecting $\boldsymbol{a}$ is $\prod_{\forall b\in\mathscr{B}} \Pi_{b,i_b} = \prod_{\forall b\in\mathscr{B}} G_{b,i_b}(\hat{\boldsymbol{u}}_b)$, which can be simplified as $\Pi_{\boldsymbol{a}}$ in (6).

Following the notation in [104, Chapter 7] we define a Gibbs field with a set of cliques $\mathscr{B}$, a configuration space with a finite size $\mathscr{V} = \prod_{\forall b\in\mathscr{B}} \mathscr{V}_b$, a set of finite potentials $\{\hat{\boldsymbol{u}}_b(v_k), \forall v_k \in \mathscr{V}_b\}_{\forall b\in\mathscr{B}}$, and a probability distribution $\boldsymbol{\Pi} = (\Pi_v, \forall v \in \mathscr{V})$, where $\Pi_v = \exp(\kappa \hat{u}(v)) / \sum_{\forall \boldsymbol{v}'\in\mathscr{V}} \exp(\kappa \hat{u}(v'))$ and $\hat{u}(v) = \sum_{b\in\mathscr{B}} \hat{\boldsymbol{u}}_b(v_k)$ with $v = (v_1, \ldots, v_{|\mathscr{B}|})$. Suppose that the configuration $v(t)$ at time instant t changes to the configuration $v(t+1)$ at time instant $t+1$ following the probability distribution $\boldsymbol{\Pi}(t)$. Hence, the evolution of the configurations in the above Gibbs field is equivalent to a Markov chain [104, Chapter 7, Theorem 2.1]. The evolution follows a time-inhomogeneous Markov chain as the configuration space $\mathscr{V}$ is finite at any time instant t. Furthermore, due to the fact that the potentials are finite, $\boldsymbol{\Pi}(t) \succ 0$ holds. Therefore, all configurations have self-loops with positive probability and thus, the Markov chain is aperiodic. Furthermore, since $\boldsymbol{\Pi}(t)$ is a positive vector, $\Pr(v(t+1) = v'' | v(t) = v') > 0$ for any $v', v'' \in \mathscr{V}$. This verifies that the process starts from configuration v' and ends in configuration v'' with a positive probability, in which the irreducible and positive recurrence properties hold. Since the time-inhomogeneous Markov chain is aperiodic, irreducible and positive recurrent, its transition probability $\boldsymbol{\Pi}$ converges to a stationary distribution as $t \to \infty$ [104, Chapter 7, Theorem 3.1].

It is shown that the transition probability of the above Gibbs field is equivalent to the action selection probability provided by Algorithm 2.1. Since the transition probability converges to a stationary distribution, the distribution $\boldsymbol{\Pi}$ given in (6) becomes stationary as well. □

Note that for a fixed κ, the algorithm converges to the stationary distribution $\boldsymbol{\Pi}$ as shown in Theorem 1, and thus the temperature parameter κ affects the optimality of the solution as the algorithm converges to $\boldsymbol{\Pi}$. Therefore, we define $\boldsymbol{\Pi}^{(\kappa)}$ as the solution given the value of κ. In the following, we show that as κ approaches infinity, the solution of the proposed algorithm converges to the global solution of the problem (25).

Theorem 2. As $\kappa \to \infty$,

$$\lim_{\kappa\to\infty} \Pi_{\boldsymbol{a}}^{(\kappa)} = \Pi_{\boldsymbol{a}}^{(\infty)} = \begin{cases} \frac{1}{|\mathscr{A}^*|} & \text{if } \boldsymbol{a} \in \mathscr{A}^*, \\ 0 & \text{if } \boldsymbol{a} \notin \mathscr{A}^*, \end{cases} \tag{7}$$

where $\mathscr{A}^*$ is the set of global optimal solutions of (25).

Proof. Let $\boldsymbol{a} \in \mathscr{A}^*$. Therefore, $\hat{u}_{\boldsymbol{a}} > \hat{u}_{\boldsymbol{a'}}$ for all $\boldsymbol{a'} \notin \mathscr{A}^*$. Then,

$$\begin{aligned} \Pi_{\boldsymbol{a}}^{(\infty)} &= \lim_{\kappa\to\infty} \frac{\exp(\kappa\hat{u}_{\boldsymbol{a}})}{\sum_{\forall \boldsymbol{a'}\in\mathscr{A}} \exp(\kappa\hat{u}_{\boldsymbol{a'}})} \\ &= \lim_{\kappa\to\infty} \frac{1}{|\mathscr{A}^*| + \sum_{\forall \boldsymbol{a'}\notin\mathscr{A}^*} \exp(\kappa(\hat{u}_{\boldsymbol{a'}} - \hat{u}_{\boldsymbol{a}}))} = \frac{1}{|\mathscr{A}^*|}. \end{aligned} \tag{8}$$

□

Theorem 2 shows that under a finite κ a non-optimal solution can be selected with non-zero probability. Thus, a finite κ cannot ensure an optimal selection of actions under the stationary distribution. However, the following theorem shows that the optimality of the solution increases with an increasing κ.

Theorem 3. For any optimal action $\boldsymbol{a} \in \mathscr{A}^*$, the probability of selecting the optimal solution after convergence, $\boldsymbol{\Pi}_{\boldsymbol{a}}^{(\kappa)}$, monotonically increases with κ.

Proof. The first derivative of (6) is:

$$\frac{\partial \Pi_{\boldsymbol{a}}^{(\kappa)}}{\partial \kappa} = \frac{\partial}{\partial \kappa} \frac{\exp(\kappa\hat{u}_{\boldsymbol{a}})}{\sum_{\forall \boldsymbol{a'}\in\mathscr{A}} \exp(\kappa\hat{u}_{\boldsymbol{a'}})} = \Pi_{\boldsymbol{a}} \left(\hat{u}_{\boldsymbol{a'}} - \mathbb{E}_{\boldsymbol{\Pi}^{(\kappa)}}[\hat{u}_{\boldsymbol{a'}}]\right) \tag{9}$$

where $\hat{\boldsymbol{u}} = (\hat{u}_{\boldsymbol{a}}, \forall \boldsymbol{a} \in \mathscr{A})$ is the utility estimation for the system. Since $\hat{u}_{\boldsymbol{a}} \geq \hat{u}_{\boldsymbol{a'}}$ for any $\boldsymbol{a} \in \mathscr{A}^*$ and for all $\boldsymbol{a'} \in \mathscr{A}$, $\hat{u}_{\boldsymbol{a'}} > \mathbb{E}_{\boldsymbol{\Pi}^{(\kappa)}}[\hat{u}_{\boldsymbol{a'}}]$ is true and thus, $\frac{\partial \Pi_{\boldsymbol{a}}^{(\kappa)}}{\partial \kappa} > 0$ holds, i.e. the probability of choosing the optimal action monotonically increases with κ. □

From Theorem 2 and Theorem 3, we note that the choice of κ affects the optimality of the solution as the algorithm converges to the stationary distribution. Next, we prove that selecting a large κ increases the expected utility of the system while increasing the probability of picking the optimal action.

Theorem 4. At convergence, $\boldsymbol{\Pi}^{(\kappa)}$, the expected value of the system utility $E_{\boldsymbol{\Pi}^{(\kappa)}}[\hat{u}_{\boldsymbol{a}}]$ monotonically increases with κ.

Proof. Consider the first derivative of the expected utility:

$$\frac{\partial \mathbb{E}_{\mathbf{\Pi}^{(\kappa)}}[\hat{u}_{\boldsymbol{a}}]}{\partial \kappa} = \frac{\partial}{\partial \kappa}\Big(\sum_{\forall \boldsymbol{a} \in \mathscr{A}} \Pi_{\boldsymbol{a}}^{(\kappa)} \hat{u}_{\boldsymbol{a}}\Big) = \sum_{\forall \boldsymbol{a} \in \mathscr{A}} \Pi_{\boldsymbol{a}}^{(\kappa)} \hat{u}_{\boldsymbol{a}} (\hat{u}_{\boldsymbol{a}} - \mathbb{E}_{\mathbf{\Pi}^{(\kappa)}}[\hat{u}_{\boldsymbol{a}}])$$
$$= \mathbb{E}_{\mathbf{\Pi}^{(\kappa)}}[(\hat{u}_{\boldsymbol{a}})^2] - \mathbb{E}^2_{\mathbf{\Pi}^{(\kappa)}}[\hat{u}_{\boldsymbol{a}}] = \mathbb{E}_{\mathbf{\Pi}^{(\kappa)}}[(\hat{u}_{\boldsymbol{a}} - \mathbb{E}^2_{\mathbf{\Pi}^{(\kappa)}}[\hat{u}_{\boldsymbol{a}}])^2]. \tag{10}$$

Here, $\mathbb{E}_{\mathbf{\Pi}^{(\kappa)}}[(\hat{u}_{\boldsymbol{a}} - \mathbb{E}^2_{\mathbf{\Pi}^{(\kappa)}}[\hat{u}_{\boldsymbol{a}}])^2]$ is the variance of $\hat{\boldsymbol{u}}$ and $\mathbf{\Pi}^{(\kappa)}$, and thus, $\frac{\partial}{\partial \kappa}(\mathbb{E}_{\mathbf{\Pi}^{(\kappa)}}[\hat{u}_{\boldsymbol{a}}]) > 0$ holds. □

Based on the above theorems, the choice of large κ ensures close global optimality. However, a large κ leads Algorithm 2.1 to exploit a single action from the beginning $(t = 1)$ and thus, exploring the rest of the actions is avoided. Therefore, κ needs to be bounded for practical implementations.

3 Dedicated spectrum sharing

In this chapter, we focus on the dedicated spectrum sharing case. Each MNO has its own dedicated spectrum it is willing to share. An MNO enables spectrum sharing when an SCN is not using 100% of its spectrum. A given SCN does not fully utilize its spectrum when it can provide the required data rate for all the users without using 100% of its spectrum, i.e., the minimum spectrum usage by SCN is ensured by utilizing the maximum transmission power and the highest order modulation and coding scheme (MCS) possible for all transmissions. From an energy efficiency perspective, it may be beneficial for an SCN to utilize its full spectrum for all transmissions. However, from spectrum sharing point of view, it is more beneficial to keep the spectrum usage to a minimum. Typically, SCNs are placed in densely populated environments without frequency planning, and have time-variant traffic profiles. The aim is to use the spectrum more efficiently in order to reduce future spectrum requirements and increase the capacity of small cell networks.

3.1 Link model

The link model[2] between an SCN and a user is illustrated in Fig. 4. A link-to-system (L2S) interface is used in the simulations. Each user is paired to the SCN based on the path loss model [105]. A geometry-based stochastic channel model (GSCM) [106, 107] is used to model fast fading and shadowing losses for all links. Channel parameters are determined stochastically, based on the statistical distributions extracted from channel measurements [106]. SCN related assumptions for the links are adopted from [105]: all links are assumed to be non-line-of-sight (NLOS) and the users are always inside buildings.

A user estimates channel-quality indicator (CQI) information, i.e., quantized signal-to-interference-plus-noise ratio (SINR), from the received signal for every physical resource block (PRB) and sends it to the SCN. The uplink channel is assumed to be ideal, i.e., error free. In order to model a practical closed loop system, periodic and delayed CQI is assumed. At the SCN, the proportional fair scheduler utilizes CQI information in the allocation of frequency resources to the most suitable users. After scheduling,

[2]The same link model is also used in Chapter 4.

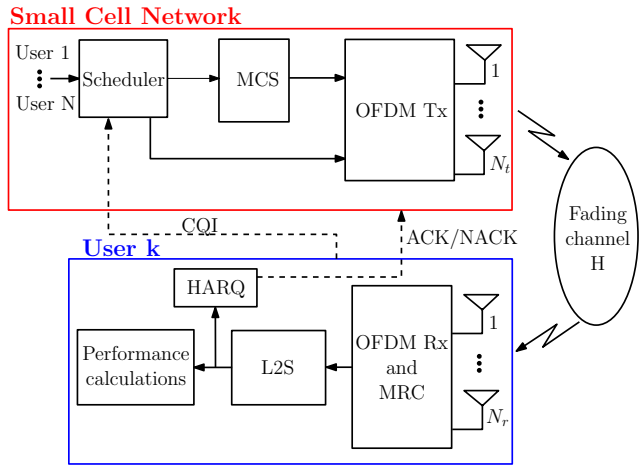

Fig. 4. Block diagram of the link model. [85] © 2015 IEEE.

the link adaptation is performed for scheduled users by selecting the MCS based on CQI information. Finally, the data is sent over the fading channel. The cyclic prefix is assumed to be longer than the multipath delay spread, and thus inter-symbol-interference is not considered.

At the receiver, perfect frequency and time synchronization is assumed. Link-to-system mapping is performed using mutual information effective SINR mapping (MIESM) [108]. This significantly reduces the computational overhead in comparison to the exact modeling of the radio links, while still providing sufficiently accurate results. In the L2S interface, SINR is calculated and mapped to the corresponding average mutual information. Based on the MIESM value, the frame error probability (FEP) is approximated according to a predefined frame error rate (FER) curve of the used MCS. Based on the FER, successful and erroneous frames can be detected, and hybrid automatic repeat request (HARQ) can take the control of retransmissions. An acknowledgement (ACK) or a negative acknowledgement (NACK) message is sent back to the SCN to signal the success or failure of the transmission, respectively. The results are obtained by simulating a predefined number of channel samples.

3.2 System model for dedicated sharing

Consider the downlink of an orthogonal frequency-division multiple access (OFDMA) SCN where $\mathscr{B} = \{1, \cdots, B\}$ SCNs are deployed. Each SCN has N_{t} transmit antennas

(Tx), which serve K users each with N_{r} receive antennas (Rx). The frequency domain resource consists of N_{c} subcarriers, where 12 subcarriers are forming a PRB. It is assumed that the spectral allocations of the SCNs are orthogonal to the macro network layer and thus only the small cell traffic is modeled. The total system bandwidth is 10 MHz at 2 GHz center frequency and it is equally divided among the MNOs.

In the system model interactions between SCNs can be modeled as graphs. It is assumed that the SCNs communicate with each other if the distance is less than or equal to 50 meters. Let $G_v = (B_v, E_v)$ denote the graph, where $v = [0, \ldots, V]$ is the number of graphs, the number of vertices in the graph (in this case SCNs) is $B_v = \{b_0, \ldots, b_n\}$ and the edges in the graph (b_i is connected to SCN b_j) are $E_v = \{(b_i, b_j)\}$. Let $\mathscr{L} = \{1, \ldots, L\}$ denote the set of MNOs. We define a function MNO$(\cdot)$, which maps SCN b_i to the respective operator, i.e., $\forall b_i, \mathrm{MNO}(b_i) \in \mathscr{L}$.

If a graph has n vertices we have an $n \times n$ matrix $\mathbf{A}$ that is called an adjacency matrix. The matrix $\mathbf{A}$ is defined by

$$\mathbf{A}_{ij} = \begin{cases} 1 & \text{if } \mathrm{SCN}_i \leftrightarrow \mathrm{SCN}_j \\ 0 & \text{otherwise} \end{cases} \tag{11}$$

where i and j are SCNs' indices. When $\mathbf{A}_{ij} = 1$, SCN_i and SCN_j communicate successfully with one another. This matrix is formed by the central controller v_0 when each SCN reports its adjacent vector, which indicates the wireless connections of the SCN to other SCNs. An SCN is willing to share its spectrum if it is not utilizing it fully. We define spectrum utilization $\mathrm{SU}(b_i), \forall b_i \in (B_v - v_0)$, and each MNO defines a sharing factor $S = [0, \ldots, 1]$ indicating how much it is willing to share if part of the spectrum is free.

3.3 Multi-operator coordination for spectrum sharing

The CQI is estimated from the received signal and SINR calculated for every PRB. When the SCN supports CoPSS, users have to calculate the CQI over the other operator's spectrum. Here, user equipment (UE) is required to receive/request reference signals from the other operator's SCNs. In this case a user can only receive wideband reference signals from other MNOs' SCNs, because we assume that the MNOs are not willing to share operator specific reference signals. This means that users can only estimate if there are other MNOs' SCNs nearby but they may not estimate the SINR accurately for each PRB when the spectrum is shared. We propose a CQI model in which it is

enough to know the spectrum utilization (SU) of other SCNs/MNOs in order to make an accurate CQI estimation.

Fig. 5 shows an example of CQI modeling for UE1 when CoPSS is either supported or not (utilization of the central controller is explained in Section 3.4). Each operator has a spectrum of 4 PRBs. UE1 is connected to SCN1/MNO1, UE2 is connected to SCN2/MNO2 and UE3 is connected to SCN3/MNO3. Without any sharing UE1 is not aware of any interference in the network. Let us assume that 50% of the spectrum is shared, now UE1 can access MNO2's and MNO3's resources and vice versa. Without any coordination, when UE1 calculates the SINR for the CQI reporting it assumes that 50% of its own MNO's spectrum is interference free and 50% experience interference from SCNs 2-3. UE1 also assumes that the shared PRBs of other MNOs are used when the SINR is calculated. The reason is that UE1 receives the wideband reference signals from other SCNs but it does not know whether shared resources are used or not. This means that a user effectively makes the worst-case estimate for the CQI, which gives the worst-case performance that can be achieved if the resources are used as estimated. If users could make an accurate estimation from other MNO spectrums for each PRB this assumption could be relaxed.

When there is coordination, each SCN receives the SU of other SCNs. This information is included in the wideband reference signals that the UEs request from the SCNs in the vicinity error free. In this example SCN2 and SCN3 transmit their SU to UE1. Now UE1 can estimate the channel accurately and transmit an accurate CQI to SCN1. Without any coordination UE1 would detect only two interference free PRBs, but with coordination seven interference free PRBs are detected.

In order for a UE to predict which part of the spectrum is not occupied, it has to know in which manner the SCN/MNO allocates PRBs to its users. In order to minimize signaling overhead, it is assumed in this work that each SCN/MNO starts allocating PRBs from the beginning or from the end of its spectrum. Arbitrary allocations would require detailed resource allocation information exchange, significantly increasing the signaling overhead. When a UE knows how much spectrum a SCN/MNO is willing to share and what the SU is, the UE can predict free and occupied portions of the spectrum. This way the UE can estimate the CQI more accurately.

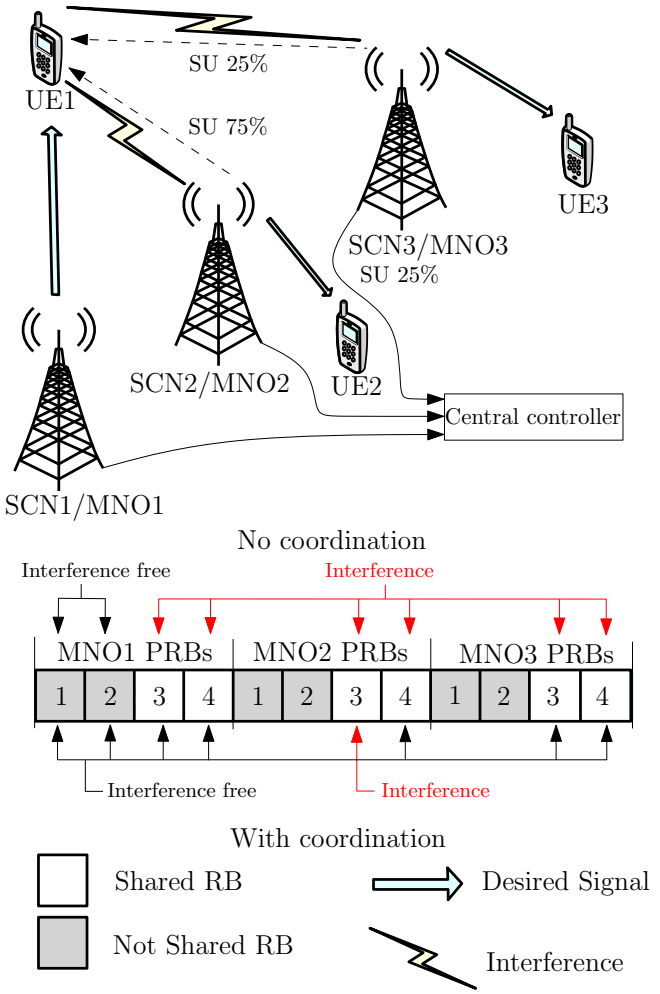

Fig. 5. CQI modeling with and without coordination between MNOs. [85] © 2015 IEEE.

3.4 Co-primary spectrum sharing algorithms for dedicated sharing

With accurate CQI estimations, we propose three centralized algorithms and one decentralized algorithm for CoPSS. The proposed algorithms use a moderate amount of shared information among MNOs/SCNs and they do not require long iterative information exchange processes. Thus, the proposed CoPSS algorithms are practical.

In Algorithm 3.1, the free shared PRBs are randomly assigned to the SCNs in the building. The idea is that the SCNs are connected to the central controller (as shown in Fig. 5) and there is no connection between the SCNs resulting a single graph G_v per building. This algorithm is time sensitive as there is a possibility that a randomly selected SCN from the graph can not exploit extra resources. Given that $b_{j'}$ is the selected SCN, the available free shared PRBs from MNO l to any SCN b_j are given by:

$$w_{jk} = \begin{cases} \lfloor \min(W_l, S) \rfloor \times Q, & \text{if } b_j = b_{j'} \\ 0 & \text{otherwise,} \end{cases} \tag{12}$$

where Q is the number of PRBs[3] and S is the sharing factor. The number of free PRBs at MNO l is defined as follows

$$W_l = 1 - \max_{b_i \in \{b | \text{MNO}(b) = l\}} \big(\text{SU}(b_i)\big). \tag{13}$$

Thus, the total number of free PRBs for SCN b_j is $\sum_{l \in \mathscr{L}} w_{jl}$.

Algorithm 3.1 Random sharing (centralized algorithm). [85] © 2015 IEEE.

1: Each SCN b_i reports its $\text{SU}(b_i)$ and sharing factor S to the central controller v_0.
2: v_0 picks $b_j \in (B_v - v_0)$ with probability $\frac{1}{|B_v - v_0|}$.
3: **if** $\text{SU}(B_j) = 1$ **then**
4: Allocate PRBs based on (12).
5: **else**
6: v_0 does not allocate any resources.
7: **end if**

In Algorithm 3.2, the free PRBs are equally assigned to overloaded SCNs in the building. It is assumed that an SCN is overloaded if the whole spectrum is utilized, i.e., the SU is one hundred percent. Sharing is performed in a centralized manner using the

[3]Notation $\lfloor \cdot \rfloor$ defines the operation of round towards negative infinity.

central controller. Therefore, we define a new set $b^+ = \{b_i | \mathrm{SU}(b_i) = 1\}$, which includes all the overloaded SCNs. Here, the free shared PRBs from MNO l to SCN b_j are

$$w_{jl} = \begin{cases} \left\lfloor \frac{1}{|b^+|} \min(W_l, S) \right\rfloor \times Q, & \text{if } b_j = b_{j'} \\ 0 & \text{otherwise,} \end{cases} \tag{14}$$

and the total amount of free PRBs for SCN b_j is $\sum_{l \in \mathscr{L}} w_{jl}$.

Algorithm 3.2 Equal sharing (centralized algorithm). [85] © 2015 IEEE.

1: Each SCN b_i reports its $\mathrm{SU}(b_i)$ and sharing factor S to the central controller v_0.
2: Central controller v_0 creates set b^+.
3: **if** $\exists b^+ \neq \emptyset$ **then**
4: Allocate PRBs based on (14).
5: **else**
6: v_0 does not allocate any resources.
7: **end if**

Algorithm 3.3 aims to share resources equally between SCNs/MNOs. The difference is that now the SCNs are not connected to the central controller, but only to the SCNs in the vicinity, i.e, sharing is done in a decentralized manner. We let $\mathscr{N}(b_i)$ denote the set of neighbor vertices of b_i and from (15) we define two different sets, $\mathscr{N}_{\mathrm{ol}}(b_i)$ for overloaded neighbors, and $\mathscr{N}_{\mathrm{nol}}(b_i)$ for not overloaded neighbors,

$$\mathscr{N}(b_i) = \{b | b \in B_v, (b, b_i) \in E_v\}, \tag{15}$$

$$\mathscr{N}_{\mathrm{ol}}(b_i) = \{b | b \in \mathscr{N}(b_i), \mathrm{SU}(b) = 1\}, \tag{16}$$

and

$$\mathscr{N}_{\mathrm{nol}}(b_i) = \{b | b \in \mathscr{N}(b_i), \mathrm{SU}(b) < 1\}. \tag{17}$$

From (16), we define a set of MNOs, which are overloaded neighbors and rest of the MNOs are not overloaded as

$$\hat{\mathscr{L}}_i = \{\mathrm{MNO}(b) | \mathrm{MNO}(b) \in \mathscr{L}, b \in \mathscr{N}_{\mathrm{ol}}\}, \tag{18}$$

and

$$\check{\mathscr{L}}_i = \mathscr{L} \backslash (\hat{\mathscr{L}}_i \cup \{\mathrm{MNO}(b_i)\}), \tag{19}$$

respectively. Now we can define the free shared PRBs w_j from the neighbors $\check{\mathscr{L}}_i$ to SCN b_j,

$$w_j = \sum_{\forall l \in \check{\mathscr{L}}_i} \left\lfloor \frac{\min\left(1 - \max_{\substack{b \in \mathscr{N}_{\text{nol}}(b_i) \\ \text{MNO}(b)=l}} \left(\text{SU}(b)\right), S\right) \times Q}{|\hat{\mathscr{L}}_i \cup \{\text{MNO}(b_i)\}|} \right\rfloor . \tag{20}$$

Algorithm 3.3 Connection based sharing (decentralized). [85] © 2015 IEEE.

1: Each b_i reports $\text{SU}(b_i)$ and sharing factor S to all b_j s.t. $b_j \in B_v$ and $(b_i, b_j) \in E_v$.
2: Each b_i analyzes received reports.
3: **if** $\text{SU}(b_i) = 1$ **then**
4: **if** $\mathscr{N}(b_i) = \emptyset$ **then**
5: b_i allocates $|\mathscr{L} \backslash \text{MNO}(b_i)| \times Q$ PRBs.
6: **else**
7: Allocate PRBs based on (20).
8: **end if**
9: **end if**

Fig. 6 shows an example of how resources are shared. It is assumed that each MNO has its own index and based on the index it knows which part of the spectrum resources can be taken from. In this example, 50% of MNO3 spectrum is free. MNO1 knows that half of the shared resources can be utilized, in this case PRB3. Similarly MNO2 knows that PRB4 can be utilized. Based on the number of overloaded SCNs/MNOs, the unused portion of the spectrum is divided equally. Allocations are interference free for each SCN/MNO if the graph is fully connected. For example, if a connection between SCN2 and SCN3 is not present, MNO1 may utilize PRB3, but MNO2 would see that MNO3 is absent and may utilize 50% of the resources, in this case PRBs 3 and 4. This means that PRB3 is utilized by MNO1 and MNO3 causing interference.

In Algorithm 3.4, aforementioned interference problem can be avoided as each SCN reports its connections to other SCNs and SU to the central controller. The central controller then forms an adjacency matrix. Utilizing the information from the adjacency matrix the central controller can generate interference free resource allocations as illustrated in the interference avoidance step in Algorithm 3.4. Now we can define free shared PRBs w_j from neighbors to SCN b_j as

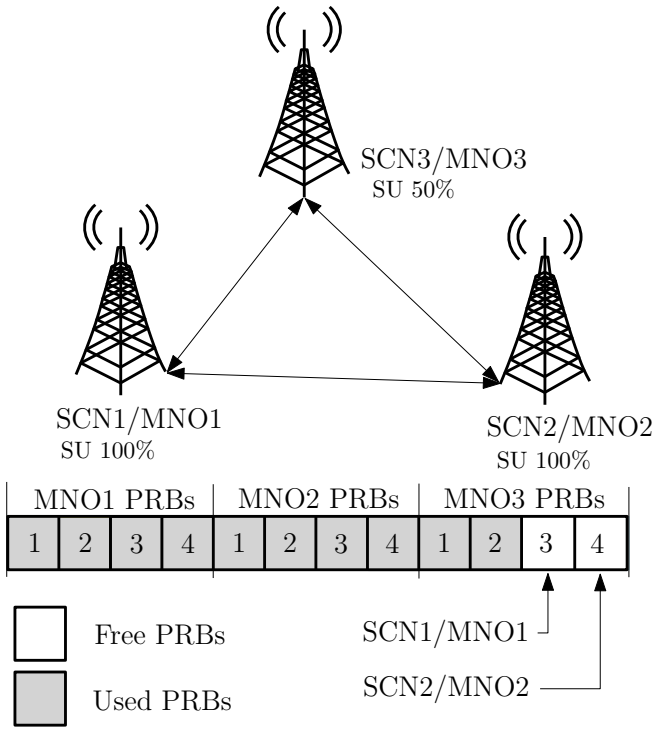

Fig. 6. Example sharing scenario for Algorithm 3.3. [85] © 2015 IEEE.

$$w_j = \sum_{\forall l \in \check{\mathscr{L}}_i} \left\lfloor \frac{\min\left(1 - \max_{\substack{b \in \mathscr{N}_{\mathrm{nol}}(b_i) \\ \mathrm{MNO}(b)=l}} \left(\mathrm{SU}(b)\right), S\right) \times Q}{|\mathscr{N}_{\mathrm{ol}}(b_i)| + 1} \right\rfloor . \tag{21}$$

The round trip-delay in the coordination methods is 5 ms and it is assumed that each MNO uses the same maximum allowed sharing percentage[4]. Backhaul links between SCNs or connections to the central controller are assumed to be ideal.

When MNOs share a common spectrum, they have to agree on the following information and rules:

– Networks operators have to share information about their network loads.

[4]Percentages could be different but results are easier to analyze when the same sharing percentage is used because we do not have to look at the gains achieved for each MNO individually.

Algorithm 3.4 Connection based sharing (centralized). [85] © 2015 IEEE.

Each SCN reports the spectrum utilization (SU), sharing percentage and adjacent vector to central controller.
Central controller forms adjacent matrix $\mathbf{A}$ and adjacent matrix of overloaded SCNs $\hat{\mathbf{A}}$.
if $\hat{\mathbf{A}} \in \mathbb{R}$ **then**
    $\exists\, b_i$ s.t. $\mathrm{SU}(b_i) = 1$.
    if $\mathscr{N}(b_i) = \emptyset$ **then**
        b_i allocates $|\mathscr{L} \backslash \mathrm{MNO}(b_i)| \times Q$ PRBs.
    else
        Allocate PRBs based on (20).
    end if
else $\hat{n}$ overloaded SCNs, $\hat{\mathbf{A}} \in \mathbb{R}^{\hat{n} \times \hat{n}}$
    PRB allocation step
    for $b_i = b_1 : b_{\hat{n}}$ **do**
        Allocate PRBs w_i based on (21).
        Remove allocated PRBs from the available free resources.
    end for
    Interference avoidance step
    for $w_i = w_1 : w_{\hat{n}}$ **do**
        $w_i \leftarrow w_i \backslash (w_i \cap w_j), j = 1, \ldots, \hat{n}, j \neq i.$
    end for
end if

– Trigger mechanism to free the spectrum if an MNO needs its own spectrum while it is utilized by the other MNO(s).
– How can the MNO benefit from the spectrum sharing?
– What is the granularity of the spectrum that can be shared?

3.5 System level performance results for dedicated spectrum sharing

System level simulations are particularly useful for studying network related issues such as resource allocation, interference management and mobility management. The extensive downlink system level simulator used in this thesis has been successfully utilized in the validation of ITU's International Mobile Telecommunications-Advanced (IMT-A) system as a part of WINNER+ group research project. The system level simulator follows the IMT-A guidelines specified in [109] and utilizes WINNER II channel model implementation [110] and parametrization [106]. In [111, 112], the simulator has been calibrated and rigorously evaluated in selected macrocell and microcell environments at 2 GHz. Moreover, the simulator has been extended to incorporate indoor femtocells, calibrated and verified in [113] and utilized in [87, 88, 114–118]. This simulator has been modified in order to support 5G related simulations, such as spectrum sharing and vehicular simulations. 5G related system level simulations will also be necessary in the future because we can not only rely on analytical analysis. Furthermore, when the simulation platform follows the standardization it can provide reliable results on the expected performance.

3.5.1 Network layout

Small cell layouts[5] are shown in Figs. 7 (fixed layout) and 8 (random layout). The building has one open corridor across it and in total 20 rooms, of size 24 m $\times$ 24 m. The internal wall attenuation is 5 dB per wall.

When the locations of the SCNs are fixed, they are placed in the center of the building and each MNO has one SCN per building, while users are evenly distributed and each of them is connected to their own MNO's SCN. When the SCNs are randomly distributed, the number of SCNs in the building is based on the deployment probability. In this layout users are located a maximum of 20 m from the SCN (inner circle). In both

[5]The same layouts are also used in Chapter 4.

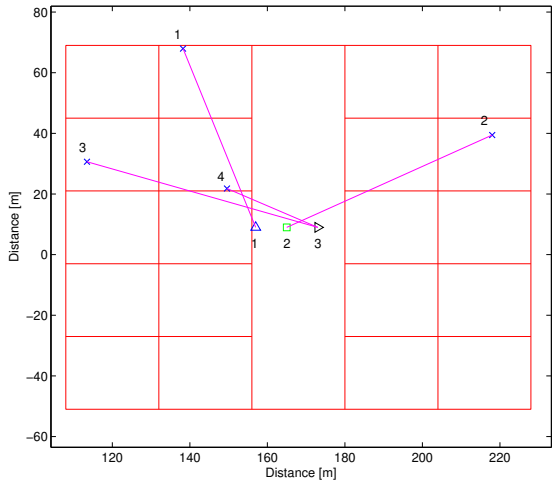

Fig. 7. Small cell layout where base stations are collocated in fixed central positions. [85] © 2015 IEEE.

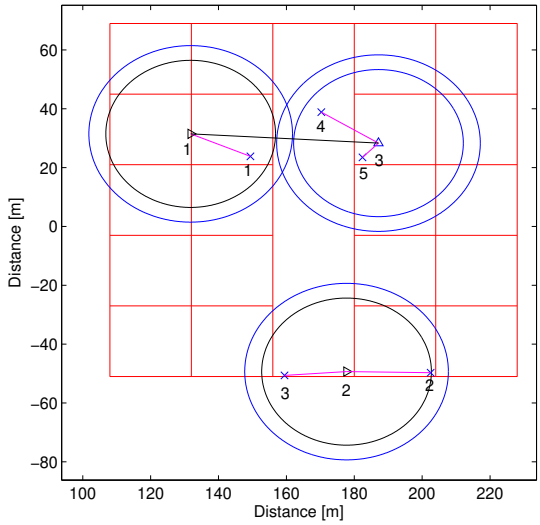

Fig. 8. Small cell layout where base stations are located randomly. [85] © 2015 IEEE.

Table 1. Simulator parameters and assumptions for a dedicated spectrum sharing scenario. [85] © 2015 IEEE.

Parameter	Assumption
Simulation direction	Downlink
Duplex mode	FDD
System bandwidth	10 MHz (divided equally between MNOs)
Number of PRBs	16 per SCN/MNO
Number of users	1-2 per SCN
Antenna configurations	1 transmitting and 2 receiving antennas
Receivers	maximum ratio combining (MRC)
HARQ	Chase combining
SCN transmission power	20 dBm
Feedback CQI period	6 ms
Feedback CQI delay	2 ms
Traffic models	**Full buffer** (10% full buffer traffic) and **Continuous constant rate transmission** (50% constant rate traffic and 40% multimedia stream traffic)
Internal wall attenuation	5 dB

layouts, the number of users connected to each SCN varies between one and two. The main reason for using two different layouts is to illustrate the applicability of the CoPSS concept in both planned (fixed) and unplanned (random) SCN deployment scenarios.

In the simulations, two different traffic models are used, full buffer and continuous constant rate transmission. With continuous constant rate transmission, two different target bit-rates are used; 4 Mb/s target rate is referred to as multimedia stream (e.g., on-demand video service) and 1 Mb/s target rate is referred to as a constant rate (e.g., users with a limited speed data connection).

Table 1 summarizes some simulation parameters and assumptions which are used throughout the simulations. Traffic in the network is constant, and the movement of users is not modeled. This means that a delay does not have a big impact on the performance because SCN resource allocation stays quite consistent throughout the simulations.

Algorithms 3.1-3.3 are used for both network layouts and Algorithm 3.4 is only used for the random layout[6]. For each CoPSS algorithm, the aim is to allocate only shared resources that are unused within the network. It should be noted that CoPSS is

[6]For the simplicity, in the results section algorithms are referred with numbers 1 to 4

highly sensitive to the network load and to different traffic types. In these simulations the network load (1-2 users per SCN) is relatively low, however at a high network load (i.e., all resources utilized) Algorithms 3.1 - 3.3 in the fixed layout and Algorithms 3.1 - 3.2 in the random layout would not provide any gain because only unused PRBs are shared between MNOs/SCNs. The reason for zero gains in the fixed layout is that when all resources are utilized, and all MNOs are collocated (12), (14) and (20) are always equal to zero. Similarly, (12) and (14) are equal to zero in the random layout. However, the graphs in the random layout can have MNOs that are not collocated and thus, (20) and (21) provide non-zero gains.

3.5.2 Coordination in the spectrum sharing

Fig. 9 shows the cumulative distribution functions (CDFs) of the SINR as estimated for the CQI with and without coordination, and as experienced at the receiver, when 50% of the spectrum is shared. The SINR in the CQI and in the receiver is the mean SINR over the allocated PRBs. It is assumed that the UE can report the PRB based CQI information. The SCN averages out the SINR with allocated PRBs and then selects a matching MCS level for transmission. The CDF shows that when the users are able to receive information about the spectrum utilization of other SCNs/MNOs in the vicinity the SINR, increases by 3 dB (between 0.05 and 0.4 in the CDF curve).

In Fig. 9, it can be seen that the SINR at the receiver saturates around 28 dB. The reason for this is that on the receiver side, error vector magnitude (EVM) is used to model hardware imperfection, which is assumed to have a value of 4%. The EVM error for the received SINR can be written as:

$$SINR_{\text{out}} = 1/\Big((1/SINR_{\text{in}}) + (EVM_{\%}/100)^2\Big) \tag{22}$$

where $SINR_{\text{in}}$ is the received SINR in linear scale and $EVM_{\%}$ is the percentage EVM.

Fig. 10 shows the mean throughput when the sharing percentage is increased from 0% to 100% with and without CQI coordination. The used CoPSS algorithm is an equal sharing algorithm. The SCNs are fixed in the center of the building. The results show that when the sharing percentage is increased and there is no CQI coordination, the achieved mean throughput starts to decrease particularly for the full buffer and multimedia stream users. When 100% of the spectrum is shared full buffer and multimedia stream users achieve a throughput of 1 Mb/s, i.e., with a 5 Mb/s loss for the full buffer users and a 2.5 Mb/s loss for the multimedia users compared with the case when 0% of the spectrum is

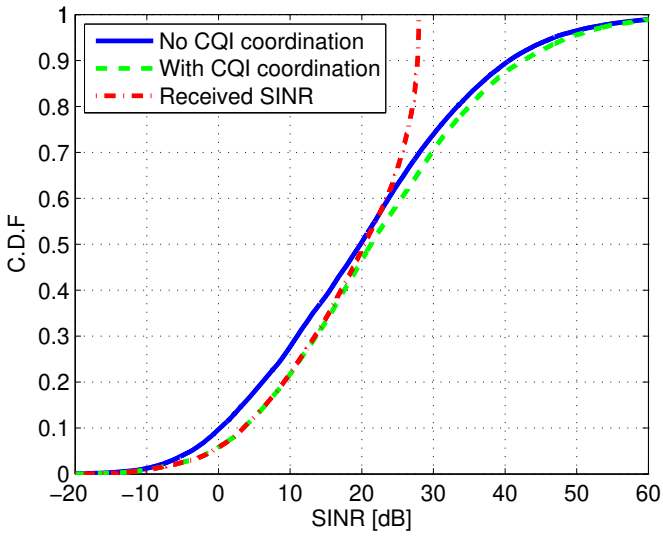

Fig. 9. UEs SINR with and without CQI coordination and in the receiver when the fixed layout is used. [85] © 2015 IEEE.

shared. When 100% of the spectrum is shared the equal CoPSS provides a 3.8 Mb/s increase in the mean throughput for full buffer users when compared to the case without the CoPSS. When the sharing percentage is increased and there is CQI coordination, the multimedia stream and the constant rate users do not achieve any gain in the mean throughput because most of the users can achieve the target bit rate, i.e., achieved throughput gain averages out. The CDFs of the throughput are analyzed in Section 4.3.

Fig. 11 shows the mean throughput results when SCNs are randomly distributed in the building. The results show that when the sharing percentage is increased and there is no CQI coordination, the achieved mean throughput for full buffer users starts to increase, but for the multimedia stream users there is a reduction in the throughput. The reason is that for full buffer users the huge increase in available PRBs outweighs the loss from the underestimated CQI, but for the lower data rate users the underestimation of the CQI leads to throughput reduction when the sharing percentage is increased. When 100% of the spectrum is shared with CQI coordination the equal CoPSS provides a 9.0 Mb/s increase in the mean throughput for full buffer users, when compared to the case without sharing.

These results show that coordination is needed between MNOs if CoPSS is supported in the network. Without coordination, the quality of the service can not be guaranteed

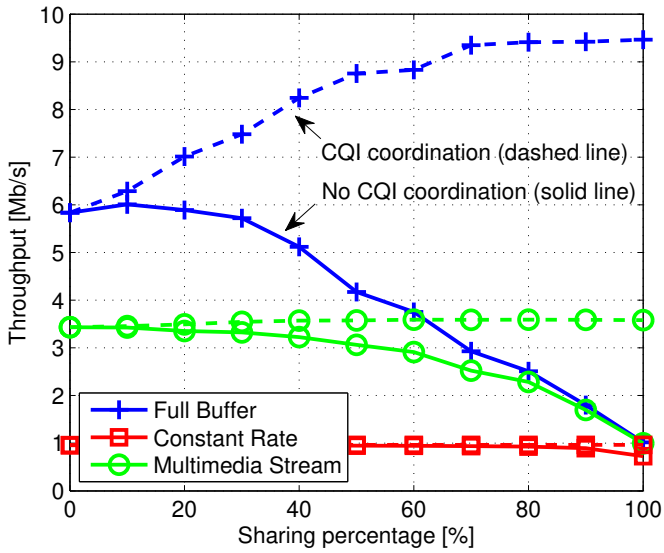

Fig. 10. Throughput with the sharing percentage, with and without CQI coordination when small cells are in fixed positions. [85] © 2015 IEEE.

and CoPSS can even result in a loss in performance. In the rest of the discussion it is assumed that there is coordination between nearby MNOs/SCNs.

3.5.3 Spectrum sharing in the fixed network layout

First the different CoPSS algorithms are analyzed in the fixed network given in Fig. 7 where all the SCNs are collocated and interconnected, i.e, there is a simple complete graph G_v per building. In this network layout, it is crucial that simultaneous use of the shared PRBs is avoided. Because the SCNs are close to each other the serving signal and the interference signal would have approximately the same strength, leading to a high FER. Decentralized sharing and equal sharing in the fixed layout should provide similar performance (all the SCN are collocated and interconnected) if there is a common protocol between MNOs defining how the shared resources can be utilized.

Fig. 12 shows the mean throughput for full buffer users for each CoPSS algorithm with sharing percentage from 0% to 100%. When 0% of the spectrum is shared the mean throughput is 6.0 Mb/s. It can be clearly seen that all the CoPSS algorithms result in throughput gains, increasing with the sharing percentage. As expected, Algorithm 1

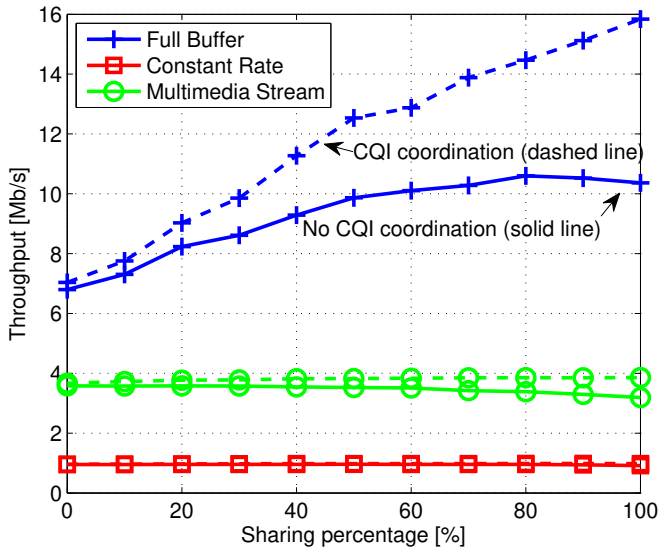

Fig. 11. Throughput with the sharing percentage, with and without CQI coordination when small cells are randomly distributed. [85] © 2015 IEEE.

provides the lowest gain, a 1.5 Mb/s increment to the mean throughput when 100% of the spectrum is shared. Algorithm 2 provides a 3.7 Mb/s gain. As mentioned in Section 3.4, Algorithm 2 and Algorithm 3 provide very similar performances because each SCN has the same knowledge as the central controller.

CoPSS provides substantial gains for full buffer users. Figs. 10 and 11 imply that only full buffer users achieve some gain from CoPSS. Figs. 13 and 14 show the CDF of the throughput for the constant rate and multimedia stream users when 50% of the spectrum is shared. From these figures, it can be seen that all the CoPSS methods provide gains over the case when the spectrum is not shared, and this applies to users with all traffic types. Fig. 14 shows, for example, that at the 20% point on the CDF there is a 0.7 Mb/s gain in throughput when Algorithm 3 is compared to no spectrum sharing.

Fig. 15 shows the CDF of the throughput for full buffer users. The theoretical maximum throughput of a user (when the SCN is only serving one user with the highest MCS level) is around 10 Mb/s. The CDF shows that a user will achieve a throughput of 10 Mb/s with a probability of 18%. For example at the 90% point on the CDF the achieved gains are; 2.0 Mb/s for Algorithm 1, 5.8 Mb/s for Algorithm 2, and 5.7 Mb/s for Algorithm 3. When compared to the theoretical maximum throughput of 10 Mb/s

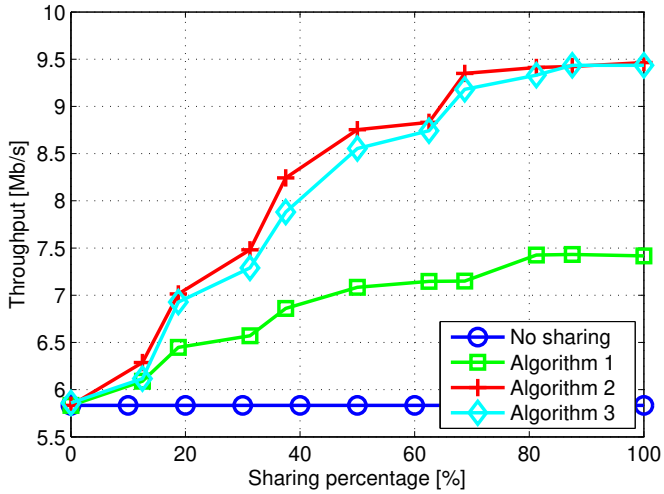

Fig. 12. Comparison of the different CoPSS algorithms in the fixed network layout. [85] © 2015 IEEE.

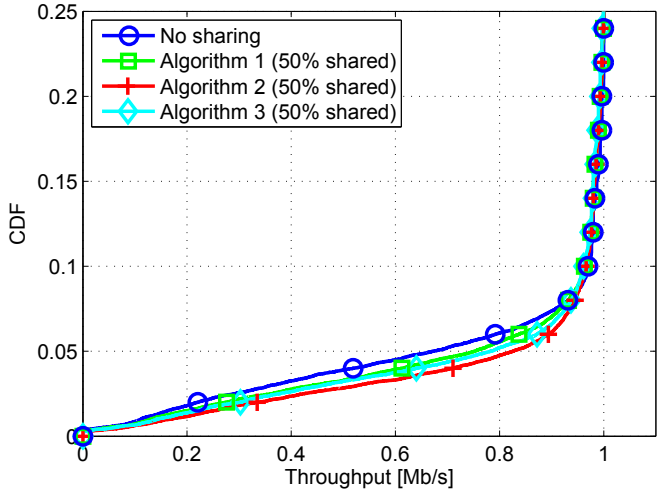

Fig. 13. CDF of constant rate user throughput for different CoPSS algorithms in the fixed network layout. [85] © 2015 IEEE.

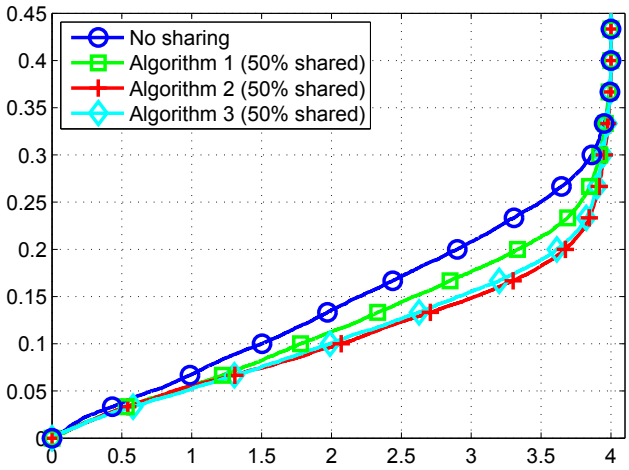

Fig. 14. CDF of multimedia stream user throughput for different CoPSS algorithms in the fixed network layout. [85] © 2015 IEEE.

Table 2. Cell edge user throughput gain [Mb/s] with the CoPSS in the fixed layout. [85] © 2015 IEEE.

Algorithm	Constant rate	Multimedia stream	Full buffer
1	0.080	0.180	0.096
2	0.154	0.159	0.327
3	0.110	0.265	0.261

without sharing, the gains are significant. Table 2 summarizes the achievable gains of cell edge users (5% from CDFs) when the CoPSS is supported.

3.5.4 Spectrum sharing in the random network layout

In the random layout (Fig. 8), a connection is formed when the coverage area of two SCNs overlap with one another, in this case a maximum distance range of 20 m + 5 m is used. It is assumed that within this distance, if the same resources are used, users will experience high interference from the neighboring SCNs. When users are within a 20 m range, the SCN acts as a local hotspot, and allows for higher data rates and spectral efficiency resulting in a better user experience. When an SCN does not detect

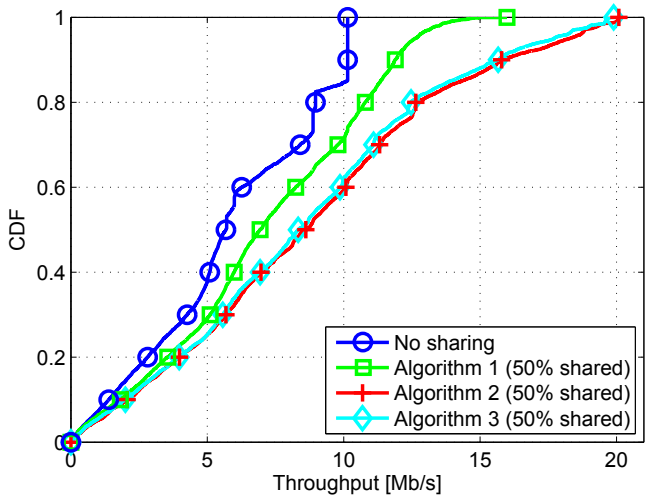

Fig. 15. CDF of Full Buffer user throughput for different CoPSS algorithms in the fixed network layout. [85] © 2015 IEEE.

the presence of any SCNs belonging to a particular MNO within its detection range, it assumes those MNOs' resources to be free and exploitable.

Fig. 16 shows the mean throughput of full buffer users for each CoPSS algorithm with a sharing percentage from 0% to 100%. When the results are compared with the fixed layout results it can be clearly seen that the achieved rates are higher because users are now closer to the SCN. When 0% of the spectrum is shared, the mean throughput is 7.0 Mb/s. Algorithm 1 provides the lowest gain, a 5.7 Mb/s improvement to the mean throughput when 100% of the spectrum is shared, while Algorithm 2 provides an 8.8 Mb/s gain. The achieved gain from Algorithm 3 is 9.6 Mb/s, and Algorithm 4 results in the highest gain of 11.6 Mb/s. The reason that Algorithm 4 provides higher gains compared to Algorithm 3 is explained in Section 3.4 and Fig. 6.

In the fixed layout, although there are no significant gains for low-data rate users, all the CoPSS methods result in higher gains over the scenario with no spectrum sharing. In the random layout the gains from CoPSS are higher than in the fixed layout. Figs. 17 and 18 show the CDF of the throughput for the constant rate and multimedia stream users when 50% of the spectrum is shared. In Fig. 18, there is a 10% probability of achieving less than 2.6 Mb/s, which is reduced to 4% in the case of sharing (Algorithm 4).

Fig. 19 shows the CDF of the throughput for the full buffer users. At the 50% point on the CDF the achieved rates are: 7.8 Mb/s for No sharing, 10.5 Mb/s for Algorithm 1,

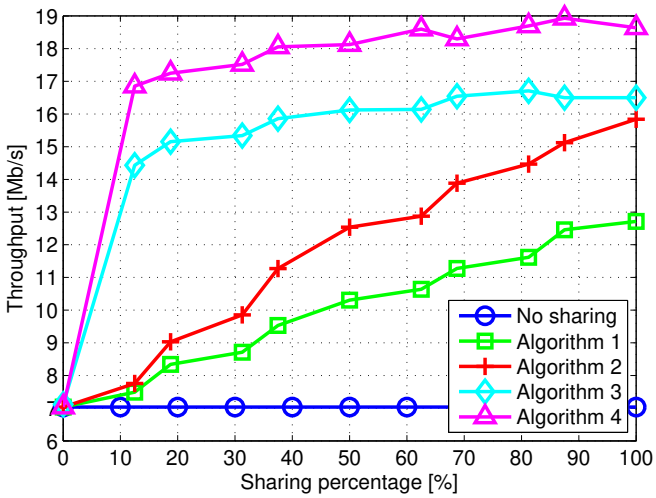

Fig. 16. Comparison of the different CoPSS algorithms in the random network layout. [85] © 2015 IEEE.

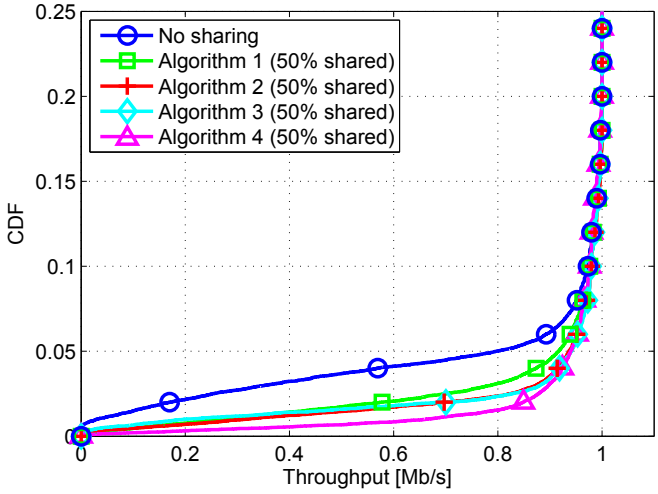

Fig. 17. CDF of constant rate user throughput for different CoPSS algorithms in the random network layout. [85] © 2015 IEEE.

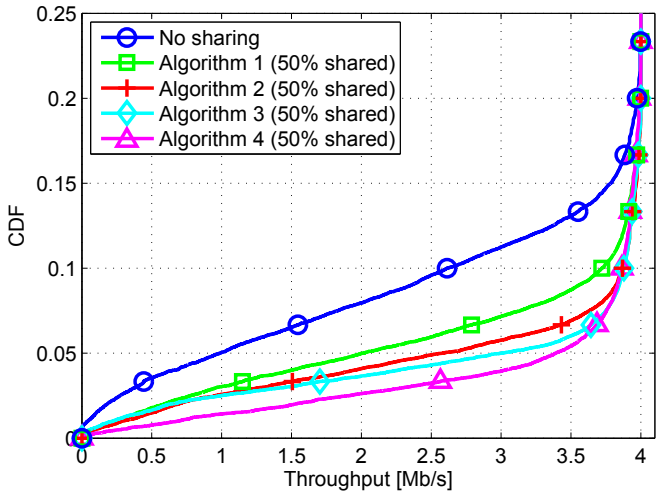

Fig. 18. CDF of multimedia stream user throughput for different CoPSS algorithms in the random network layout. [85] © 2015 IEEE.

Table 3. Cell edge user throughput gain [Mb/s] with the CoPSS in the random layout. [85] © 2015 IEEE.

Algorithm	Constant rate	Multimedia stream	Full buffer
1	0.117	1.022	1.171
2	0.137	1.594	1.811
3	0.144	2.008	1.869
4	0.141	2.403	3.129

11.6 Mb/s for Algorithm 2, 15.2 Mb/s for Algorithm 3 and 18.8 Mb/s for Algorithm 4. The achieved gains are significant compared to the no spectrum sharing scenario with a theocratical maximum of 10 Mb/s. Table 3 summarizes the gains of cell edge users when the CoPSS is supported.

3.5.5 Spectrum sharing with higher network load

As discussed earlier, a higher network load limits the achievable throughput gains using CoPSS. Table 4 shows the mean achieved throughput of full buffer users, for an increasing network load, when 100% of each MNOs spectrum is shared. The results clearly show that the gain in average throughput when utilizing CoPSS decreases with

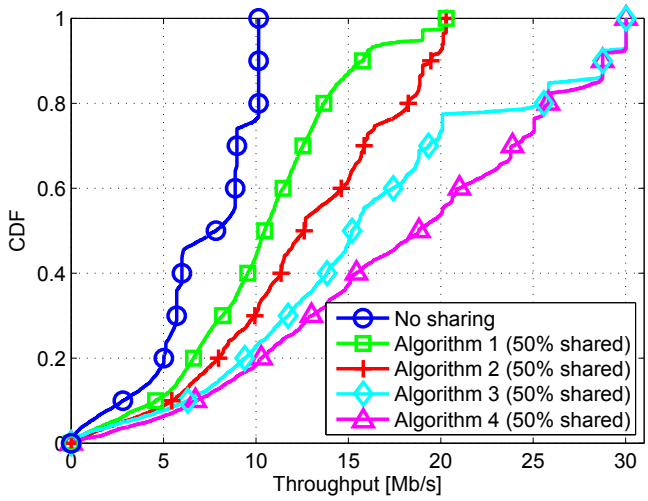

Fig. 19. CDF of full buffer user throughput for different CoPSS algorithms in the random network layout. [85] © 2015 IEEE.

Table 4. Achieved mean throughput [Mb/s] with CoPSS in the random layout with different network loads. [85] © 2015 IEEE.

Users	No sharing	Algo. 1	Algo. 2	Algo. 3	Algo. 4
1-2	7.04	12.71	15.84	16.50	18.64
1-4	4.84	9.11	10.68	11.64	13.07
1-6	3.34	6.27	7.30	9.08	9.69

the network load. However, utilizing CoPSS does result in a non-negligible increase in throughput, even in the case of a high network load.

Although Algorithm 1 is totally random, it exhibits significant throughput gains compared to the no sharing method. Thus, even a simple CoPSS can help to improve capacity in SCN network scenarios. This type of sharing does not guarantee that resources are shared equally between SCNs/MNOs during one time instant, but each SCN has an equal chance of being chosen. Algorithms 2 and 3 in the fixed network layout provide similar performance because all the SCN are collocated and interconnected. Generally, if all SCNs are connected, our proposed algorithm provides substantial throughput gains without a central controller.

In the random layout, Algorithms 2 and 3 exhibit different performances. In this case, the decentralized Algorithm 3outperforms the centralized Algorithm 2. This is because

the decentralized algorithm does not share resources equally within each building, but resources are shared between SCNs that are within communication range of one another. In this case, an isolated SCN achieves significant gains in throughput even for a low sharing percentage. When Algorithm 3 and Algorithm 4 are compared, the centralized algorithm provides better performance as explained in Section 3.4. The decentralized Algorithm 3 provides substantial gains as compared to the no sharing case, with an average gain of more than 120%. However, the centralized Algorithm 4 only results in an additional average gain of 12% over Algorithm 3. Given that the performance of the decentralized Algorithm 3 is so close to that of the centralized Algorithm 4, we conclude that Algorithm 3 is the most suitable for all the aforementioned scenarios.

The proposed algorithms do not require complex computation, or extensive signaling between SCNs. Algorithms 2 - 4 reach a stable point quickly, and the only delay is the coordination delay between SCNs/MNOs. This is because there is no requirement for any iterative information exchange between the SCNs/MNOs, due to the common rules between SCNs/MNOs, which determine how the spectrum is shared.

3.6 Summary

In this chapter, we have proposed and evaluated four different approaches toward co-primary multi-operator spectrum sharing in a small cell indoor environment with a mixed traffic distribution. A framework has been established under the system simulation platform where the system throughput performance has been rigorously assessed. The results reveal the utmost importance of channel quality signaling between MNOs to take full advantage of shared resources. When MNOs share spectrum utilization information, the channel quality can be accurately estimated. Without coordination, decent quality of service cannot be guaranteed and CoPSS can even result in a loss in performance.

Provided numerical results confirm high potential, co-primary spectrum sharing can offer to increase system throughput in the multi-operator setting. Even simple random spectrum sharing can help to improve the capacity in SCN network scenarios. The proposed decentralized algorithm provides substantial gains compared to the no sharing case, with an average gain of more than 120%. An additional gain of 12% can be achieved when resources are allocated in a centralized manner. The proposed algorithms do not require complex computation, or extensive signaling between SCNs. The proposed algorithms reach a stable point quickly, and the only delay is the coordination delay between SCNs/MNOs. Thus, the proposed CoPSS algorithms are highly practical.

A higher network load limits the achievable throughput gains using CoPSS. However, utilizing CoPSS results in a non-negligible increase in throughput even in the case of a high network load.

4 Common spectrum sharing

In this chapter, we focus on the common spectrum sharing case in which MNOs share a common pool of radio spectrum. In Chapter 3 the main focus was on possible gains in the achieved throughput when the MNOs have similar traffic patterns and spectrum sharing is done at the PRB level. Spectrum sharing at the PRB level is challenging because different OPs' SCNs have to be synchronized. However, this type of spectrum sharing guarantees more efficient utilization of the spectrum. Coarser granularity component carrier level resource sharing may be a more practical approach when multi-operator networks are not jointly synchronized. In this chapter a decentralized algorithm is introduced, where different MNOs share a common pool of component carriers (CCs) and the MNOs have different traffic requirements. We also conduct an analytical study of the proposed method. Traffic in the network is continuous with a constant rate. By minimizing a time average cost function per SCN, the long-term fairness of the spectrum sharing among the base stations is ensured. To solve the cost minimization problem per SCN in a decentralized manner with no SCN coordination, we propose CoPSS algorithms using a learning tool known as Gibbs sampling. The proposed algorithms are compared with a number of state-of the-art techniques.

4.1 System model for common spectrum sharing

Consider the downlink of an OFDMA SCN where a set of SCNs $\mathscr{B}$, operated by a set of MNOs $\mathscr{L} = \{1, \cdots, l\}$, are deployed. MNO l controls a set of its own SCNs $\mathscr{B}_l$, and thus $\mathscr{B} = \cup_{\forall l \in \mathscr{L}} \mathscr{B}_l$ with $\mathscr{B}_l \cap \mathscr{B}_{l'} = \emptyset$ for all $l \neq l'$. Each SCN $b \in \mathscr{B}$ has K users. The frequency domain resource consists of N_{c} subcarriers, where 12 subcarriers form a physical resource block (PRB) and 6 PRBs form a CC. A common pool consists of N_{cc} number of CCs. Moreover, we assume that the SCNs do not coordinate with each other.

4.2 Co-primary spectrum sharing algorithms for common sharing

We consider a CoPSS-enabled system where each MNO has its own dedicated spectrum and has access to a shared common pool of CCs as shown in Fig. 20. The main goal is to satisfy a target rate per SCN b, which is achieved by minimizing a time average cost

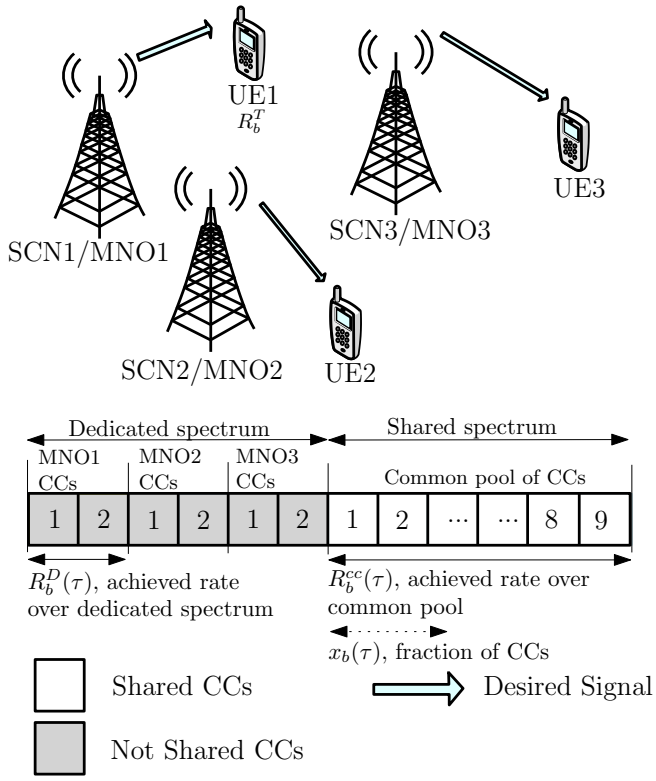

Fig. 20. System model and spectrum allocation. © 2015 [87].

function defined as follows:

$$\overline{f(t)} = \frac{1}{t}\sum_{\tau=1}^{t}\left(\frac{R_b^{\mathrm{D}}(\tau)+x_b(\tau)R_b^{\mathrm{cc}}(\tau)}{R_b^{\mathrm{T}}}-1\right)^2, \tag{23}$$

while ensuring the fairness of spectrum sharing among MNOs. Here, $R_b^{\mathrm{D}}(\tau)$ is the achievable rate of SCN b when the dedicated spectrum is used, $x_b(\tau)$ is the fraction of CCs used from the common pool by SCN b, and $R_b^{\mathrm{cc}}(\tau)$ is the summation of the bits that can be transmitted over all the CCs in the common pool. R_b^{T} is the users' sum rate target when served by SCN b.

Fig. 21 illustrates an example of the cost function shape. In this example the target rate of an SCN is 5 Mb/s and the SCN achieves a rate of 2 Mb/s. When the SCN uses a fraction of the CCs the achieved utility is close to zero and the target rate is achieved.

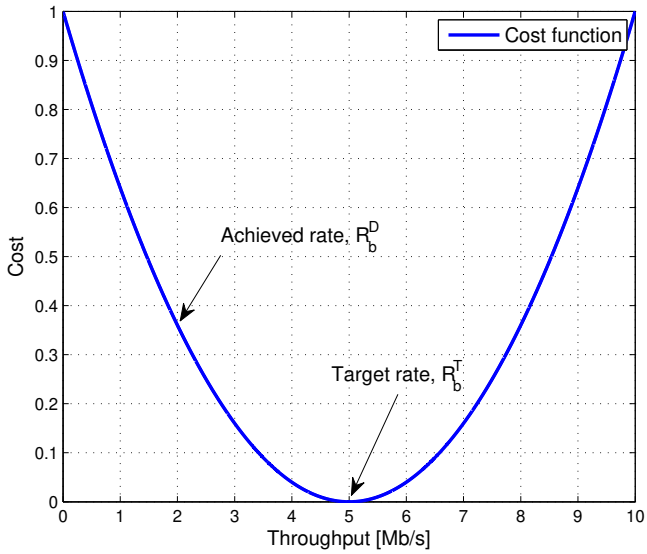

Fig. 21. Example of the cost function shape.

The cost minimization problem of SCN b is formally defined as follows:

$$\underset{\left(x_b(t),\forall t\right)}{\text{minimize}} \quad \overline{f(t)} \tag{24a}$$

$$\text{subject to} \quad \left(\frac{1}{T}\sum_{\tau=t-T}^{t} x_b(\tau) - v_{\max}\right) \leq \Delta v, \tag{24b}$$

$$0 \leq x_b(t) \leq 1, \tag{24c}$$

where $\frac{1}{T}\sum_{\tau=t-T}^{t} x_b(\tau)$ is the moving average of the spectrum usage over time window T. Parameter $v_{\max}$ is the pre-agreed maximum spectrum sharing ratio among operators, which is used to guarantee long term fairness between SCNs/MNOs[7]. Constraint (24b) allows MNOs to violate the average spectrum usage by an amount of Δv from the pre-agreed maximum spectrum sharing ratio.

[7]Parameter T has to be selected by MNOs, i.e., from minutes to days. In the simulations T is a fraction of the simulation time. Different time windows are analyzed in Section 4.3.

4.2.1 Learning algorithm

The purpose of the proposed approach is to enable SCNs to autonomously select a suitable set of CCs, $x_b(t)$, to minimize their cost functions in a decentralized manner. The variable $x_b(t)$ is referred to as the action hereinafter. However, the achievable throughput of an SCN depends not only on its own choice of action but also on the remaining SCNs due to the interference caused on the shared CCs. To address this problem we use a reinforcement learning mechanism based on Gibbs sampling [119]. This learning algorithm provides a mechanism to choose $x_b(t)$ at each time t with a given probability that depends on the estimated average rate. Moreover, the long term fairness constraint depends on all the variables $x_b(t-T),\ldots,x_b(t-1)$, which cannot be controlled at the current time instance. Therefore, we modify (24) by moving the fairness constraint as a regularization term in the cost function as follows:

$$\begin{aligned} &\underset{\left(x_b(t),\forall t\right)}{\text{minimize}} \quad \overline{f(t)} + \alpha\left(\bar{v}_b(t) - v_{\max}\right) \\ &\text{subject to} \quad 0 \leq x_b(t) \leq 1, \end{aligned} \tag{25}$$

where $\bar{v}_b(t) = \frac{1}{T}\sum_{\tau=t-T}^{t} x_b(\tau)$ is the moving time average of the spectrum usage over time window T and $\alpha \geq 0$ is the regularization coefficient of the spectrum violation.

To solve (25), we propose a learning based algorithm, where SCN b selects a suitable fraction of CCs, $x_b(t)$ which maximizes its utility

$$u_b(t) = -\left(\overline{f(t)} + \alpha\left(\bar{v}_b(t) - v_{\max}\right)\right). \tag{26}$$

Let $\pi_b(t) = [\pi_{b,1}(t),\ldots,\pi_{b,|\mathscr{A}_b|}(t)]$ be a probability distribution in which SCN b selects its ith action as $x_b(t)$ from its action space $\mathscr{A}_b = \{0, \frac{1}{N_{\text{cc}}},\ldots,1\}$ at time instant t with $\pi_{b,i}(t) = \Pr(x_b(t) = \frac{i-1}{N_{\text{cc}}})$, where $i \in \{1,\ldots,N_{\text{cc}}+1\}$.

For each action SBS b estimates its utility $\hat{u}_b(t) = [\hat{u}_{b,1}(t),\ldots,\hat{u}_{b,|\mathscr{A}_b|}(t)]$, which is the expected utility for each action over the time period $\{1,\ldots,t-1\}$. At each time t, SBS b updates its mixed strategy probability distribution $\pi_b(t)$ in which the actions with higher probabilities are exploited while exploring the actions with low probabilities. Such behavior can be captured by the Boltzmann-Gibbs (BG) distribution as shown in Chapter 2 Section 2.2.

The proposed Gibbs algorithm is summarized in Algorithm 4.1. At the beginning of each time instant t each SCN selects its action $x_b(t)$ based on its mixed strategy probability $\pi_b(t-1)$, i.e., $x_b(t)$ is a random variable with probability mass function $\pi_b(t-1)$.

Algorithm 4.1 Co-primary spectrum sharing algorithm using Gibbs sampling.

1: Each SCN b initializes its probability distribution $\pi_b(t)$ and initial utility estimations $\hat{u}_b(t)$.
2: **while** $t > 0$ **do**
3: Each SCN b selects its action $x_b(t)$ based on its mixed strategy probability $\pi_b(t-1)$.
4: Calculate objective function (25) at time t.
5: Update utility estimation and mixed strategy probability using (5).
6: $t \rightarrow t+1$
7: **end while**

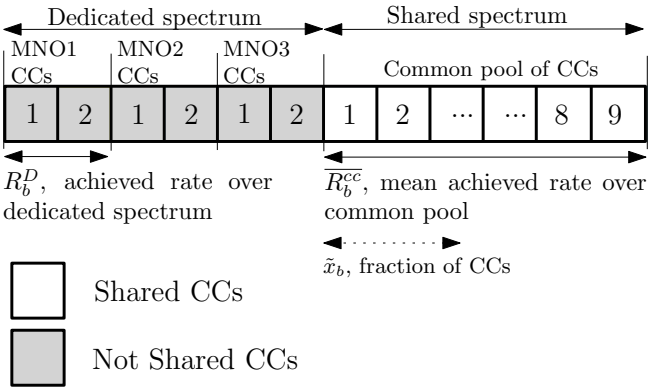

Fig. 22. Spectrum allocation with parameters for Gibbs with distribution update initialization.

4.2.2 Gibbs with distribution update initialization

In the original Gibbs algorithm, the uniform distribution over the action space is used as the initialization distribution $\pi(0)$, which is the conventional strategy when the Gibbs algorithm is applied [120]. Here, we propose a non-uniform initial distribution in order to improve the performance of the proposed learning algorithm.

The main idea is to modify the initial distribution, which is possible with an accurate CQI estimation. Specifically, each SCN estimates the number of CCs needed at the initialization such that

$$\tilde{x_b} = \frac{R_b^{\mathrm{T}} - R_b^{\mathrm{D}}}{\overline{R_b^{\mathrm{cc}}}}, \tag{27}$$

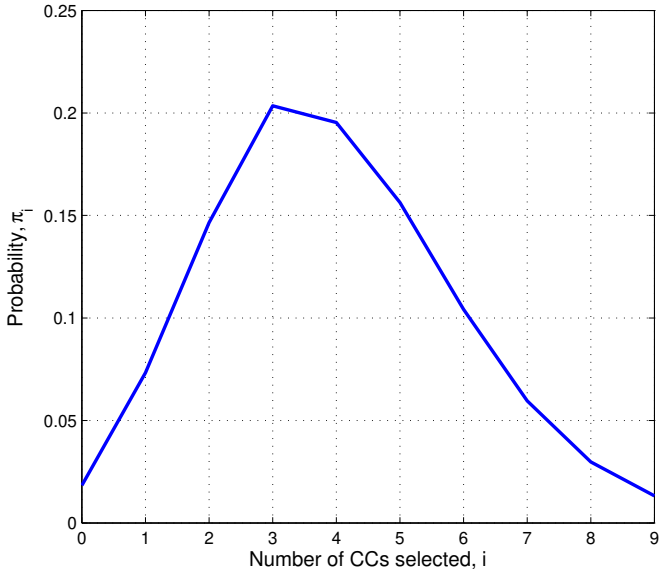

Fig. 23. Example of an initial distribution after estimation.

where R_b^{T} is the target rate, R_b^D is the achieved rate by using the dedicated spectrum and $R_b^{\bar{\mathrm{cc}}}$ is the mean value of the bits that can be transmitted over all the CCs in the common pool as shown in Fig. 22. When each SCN evaluates $\tilde{x_b}$, this information is used to calculate the modified initial distribution

$$\tilde{\pi}_{b,i} = \frac{\tilde{x}_b^i}{i!} e^{-\tilde{x}_b}, \tag{28}$$

which follows the Poisson probability mass function (pmf). However, the Poisson pmf is defined for an infinite number of discrete actions whereas the action space of SCN b is limited by finite choices. Therefore, a truncated Poisson pmf is needed. Here, we truncate the distribution by adding the tail of the original distribution to the most convenient action $\tilde{x}_b$. Modifying the uniform distribution improves the learning speed since each SCN already has some insight into which actions should be exploited. However, these SCNs can still explore the actions with low probabilities. Fig. 23 shows an example of an initial distribution after estimating how many CCs are needed. In this example the preferred number of CCs is $\tilde{x_b} = 3$.

4.2.3 Proposed algorithms and performance metrics

We propose three decentralized algorithms (Gibbs, Gibbs+penalty and Gibbs+distribution) for CoPSS and compare them with three state-of-the-art algorithms (No sharing, Greedy and Equal). The proposed decentralized algorithms do not require sharing any information between MNOs/SCNs. Thus, the proposed CoPSS algorithms are suitable for practical implementations. The baseline models and the proposed algorithms are as follows:

- *No sharing:* SCNs/MNOs do not have access to the common pool of CCs.
- *Greedy:* The first algorithm is a greedy (decentralized) algorithm, where each SCN selects a suitable set of CCs in a greedy manner. The main goal is to achieve the target rate, thus, fairness between operators cannot be guaranteed. This algorithm performs well in scenarios where SCNs are isolated, due to less interference, although the CCs are shared.
- *Equal:* The common pool of CCs is shared orthogonally and equally between operators. This algorithm performs well in scenarios where the SCNs are collocated. When SCNs are close to each other, the serving signal and the interference signal have approximately the same strength, resulting in a high FER. Thus, avoiding simultaneous use of the shared CCs is crucial.
- *Gibbs:* Solving (25) with $\alpha = 0$ using learning-based steps (4) and (5) that allows spectrum usage violations in the network.
- *Gibbs+penalty:* Solving (25) with a penalty ($\alpha > 0$) using learning-based steps (4) and (5), which allow instantaneous spectrum usage violations while maintaining long-term fairness.
- *Gibbs+distribution:* Solving (25) with $\alpha = 0$ using learning-based steps (4) and (5) that allows spectrum usage violations in the network. The main difference from the conventional Gibbs algorithm is that in the initialization phase, each SCN solves (27) and then (28) is used as its initial distribution, rather than a uniform distribution.

In the dedicated spectrum sharing case, MNOs have to agree on the following information and rules:

- What the agreed maximum sharing ratio is over the time window (for example equal amount per MNO).
- The time window length for long-term fairness (minutes/hours/days).
- The penalty for exceeding the agreed maximum sharing ratio.

If an MNO changes these values without informing others, fairness could not be guaranteed. In this case a central controller is needed that sends this information to each MNO/SCN. However, this information does not need to be updated frequently and the values could remain the same for days.

The main performance metrics are user throughput and the Jain's index [121], which is a qualitative measure of the fraction of satisfied users. Based on the achieved throughputs, which are normalized by the target rates, the Jain's index for the network is given by

$$J = \frac{(\sum_{b\in\mathscr{B}} r_b)^2}{|\mathscr{B}| \sum_{b\in\mathscr{B}} r_b^2}, \tag{29}$$

where r_b is the achieved rate per SCN b. The fairest case is when all users have the same throughput, i.e., the Jain's index equals one.

4.3 System level performance results for common spectrum sharing

In this section, a single user is connected to each SCN. Parameter R_b^{T} in (23) takes into account the demand of the users served by SCN b. Therefore, the scenario with multiple users per SCN is equivalent to a scenario with a single user per SCN with high demand. Thus, the proposed spectrum sharing algorithm is applicable for multi-user scenarios. The assumption of a single user per SCN is simply to reduce simulation time and complexity. Results are averaged out over 500 random network topologies, e.g., simulations cover sparse and dense deployments of SCNs/MNOs in the building[8].

Table 5 summarizes the main simulation parameters and assumptions used throughout the simulations. The traffic in the network is constant. Thus, delays do not have a big impact on the performance due to the consistency of SCN resource allocation throughout the simulations.

In the simulations, continuous constant rate transmission is used. We increase the MNO1 target throughput while MNO2 and MNO3 have a constant target throughput of 5 Mb/s. This allows us to analyze how different algorithms work when MNOs have similar or different traffic patterns. As already mentioned, in [85], we focused on the possible gains in the achieved throughput when MNOs have similar traffic patterns.

[8]Link model and network layout are shown in Chapther 3.

Table 5. Simulator parameters and assumptions for common spectrum sharing scenario.

Parameter	Assumption
Duplex mode	FDD
System bandwidth	20 MHz
Number of CCs	2 per MNO
Number of CCs common pool	9
Number of users	1 per SCN
Antenna configurations	1 Tx, 2 Rx
Receivers	MRC
HARQ	Chase combining
SCN transmission power	20 dBm
Feedback CQI period	6 ms
Feedback CQI delay	2 ms
Traffic model	Continuous constant rate transmission
Internal wall attenuation	5 dB
Deployment probability	0.4 $\sim$ 10 SCNs on average
Number of MNOs	3
Carrier frequency	2 GHz
Simulation time	1000 ms
Time window T	300 ms
Penalty coefficient α	4
Temperature κ_b	10
Learning rate exponents γ and ε	0.6 and 0.95

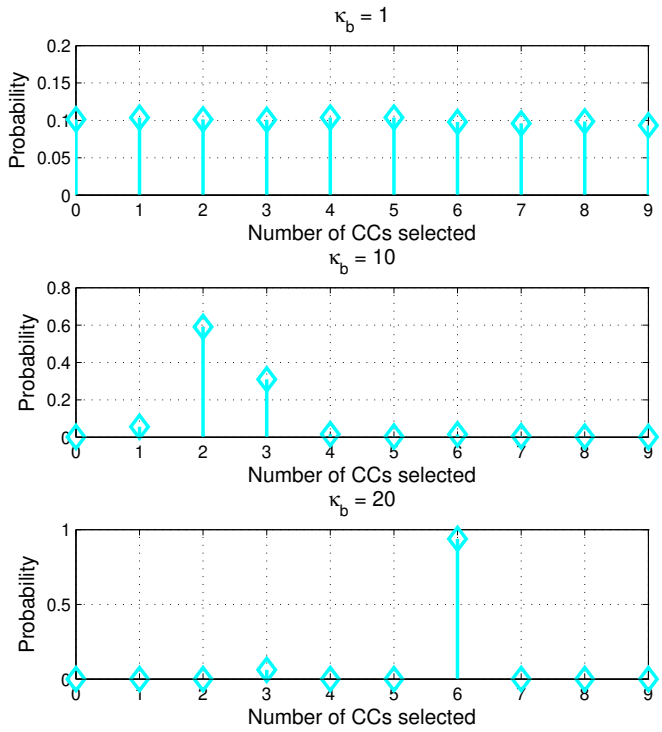

Fig. 24. Final distribution of the Gibbs algorithm with different κ_b values.

4.3.1 Parameter analysis

As mentioned in Section 4.2.1, $\kappa_b > 0$ is a temperature parameter that balances between exploration and exploitation. Fig. 24 illustrates the impact of the temperature on the resultant final distribution for three different temperature values. When $\kappa_b = 1$, the final distribution is almost uniform, which means that the temperature is too low and the algorithm does not have enough time to learn how many CCs are needed. When $\kappa_b = 20$, then the learning is too fast since the probability to select six CCs is almost equal to one (even though the best number of CCs could be even zero or nine). When $\kappa_b = 10$, this balances the exploration and exploitation, i.e., efficient learning, and the final distribution is neither uniform as with $\kappa_b = 1$ nor deterministic as with $\kappa_b = 20$.

The Gibbs+penalty algorithm includes two parameters controlling its performance, the time window T and the regularization coefficient of the spectrum violation α, which

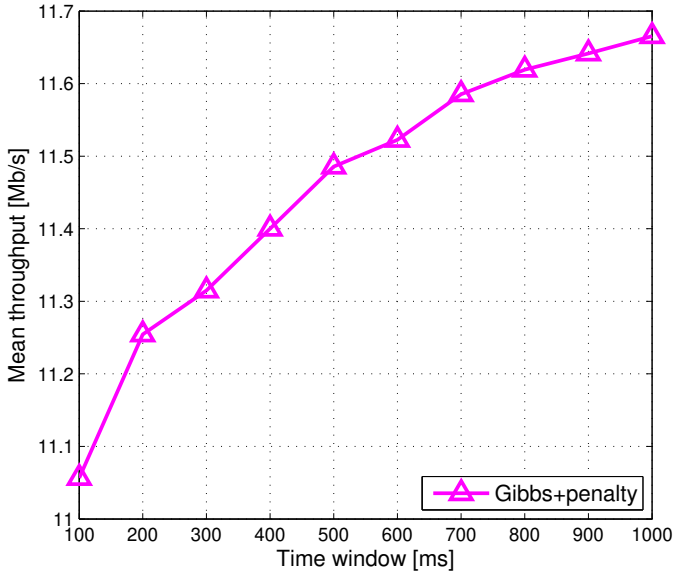

Fig. 25. Impact of time window for the Gibbs+penalty algorithm.

we will refer to as operator's penalty coefficient hereafter. First, we analyze the impact of the time window T. In Fig. 25, we show the mean throughput when the time window is increased and the simulation time is one second. In this scenario, the MNO1 target throughput is 20 Mb/s. When the time window is increased, a higher mean throughput is achieved. The reason is that when time windows are larger, MNOs have more time to violate the pre-agreed maximum sharing ratio. Based on these results, hereinafter we will use a time window of $T = 300$ ms. This allows MNOs to violate for a short period. However, as the simulation time exceeds T, SCNs start to limit the spectrum usage if they are violating the pre-agreed maximum sharing ratio. By controlling the time window, better long term fairness is achieved between MNOs.

The second parameter α, is a constant value that controls how significant the impact of the penalty coefficient is on the utility function. In Fig. 26, we can see how the achieved mean throughput decreases when the penalty coefficient is increased. For the rest of the simulations $\alpha = 4$ is used as a penalty constant that drops the mean throughput by 0.8 Mb/s when compared to the conventional Gibbs algorithm ($\alpha = 0$). Our choices of time window $T = 300$ and penalty coefficient $\alpha = 4$ ensure a sufficiently

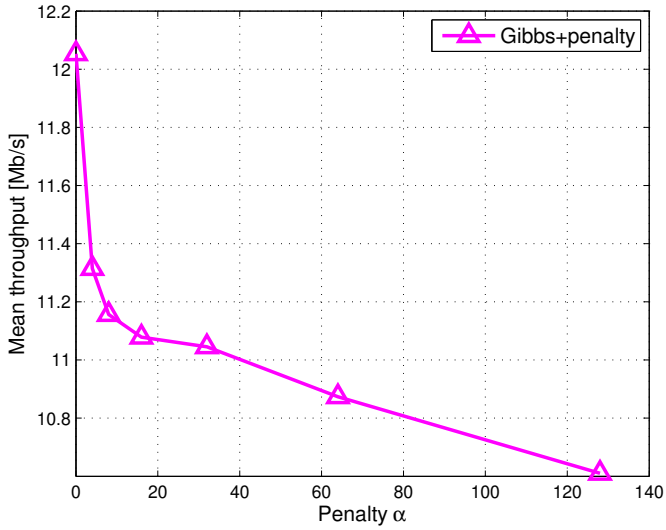

Fig. 26. Impact of the operator's penalty coefficient for the Gibbs+penalty algorithm.

large penalty term in which the proposed algorithms exhibit considerable performance differences over the conventional Gibbs algorithm.

4.3.2 Convergence analysis

Fig. 27 compares the convergence time and the achieved utility between the conventional Gibbs, Gibbs+penalty and Gibbs+distribution algorithms. For all algorithms the convergence time is similar. However, the achieved utility is higher with the Gibbs+distribution algorithm because the modification of the initial distribution improves the learning procedure. Thus, each SCN already has some insight regarding the actions to be taken even at the initial phase compared to the conventional Gibbs algorithm. However, the learning curve of the Gibbs+penalty algorithm exhibits a different behavior over the other two methods due to the impact of the penalty term. During the first 100 ms, MNOs exploit the spectrum usage to improve their throughputs by violating the spectrum sharing ratio. As the simulation time reaches the duration of the time window, these violations result in large penalties and thus, lower utility. Therefore, the MNOs have to compensate for the spectrum usage violation, which lowers the throughputs. As the

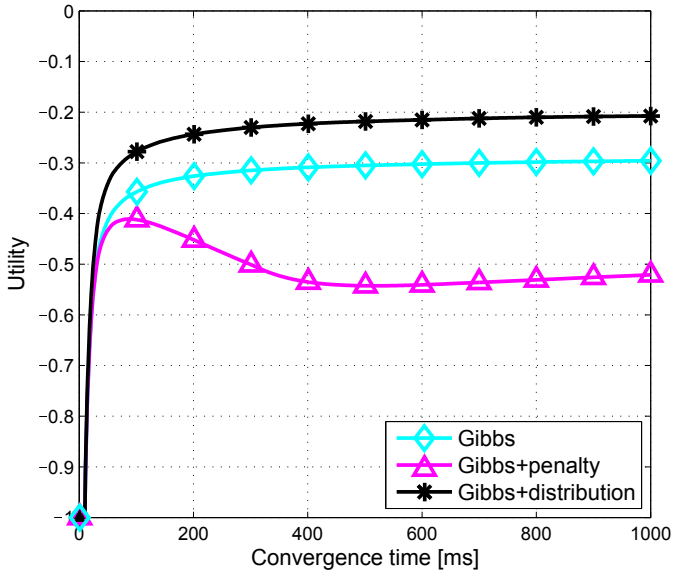

Fig. 27. Convergence time.

simulation proceeds, the MNOs discover the balance between increasing throughputs and maintaining the spectrum usage fairness in which the convergence is achieved.

4.3.3 Performance results in fixed layout

First the different CoPSS algorithms are analyzed in the fixed network. Fig. 28 shows the achieved mean throughput of MNO1 for different target rates. Here, we can capture how the CoPSS works when the MNOs have different throughput targets. In the simulations, we increase MNO1 target throughput while MNO2 and MNO3 always have a constant target throughput of 5 Mb/s. The results show that when MNO can not access the common pool of CCs the achieved throughput saturates at around 5 Mb/s. When different sharing algorithms are compared we can see that the maximum difference in the achieved mean throughput is around 1 Mb/s. Equal sharing provides the best mean throughput as expected, because there is no interference between the SCNs/MNOs.

Fig. 29 illustrates the CDF rate of MNO1 when the target rate is 30 Mb/s. The Equal algorithm saturates at around 19 Mb/s while the other algorithms provide higher throughputs and the highest throughput can be achieved when the Greedy or Gibbs

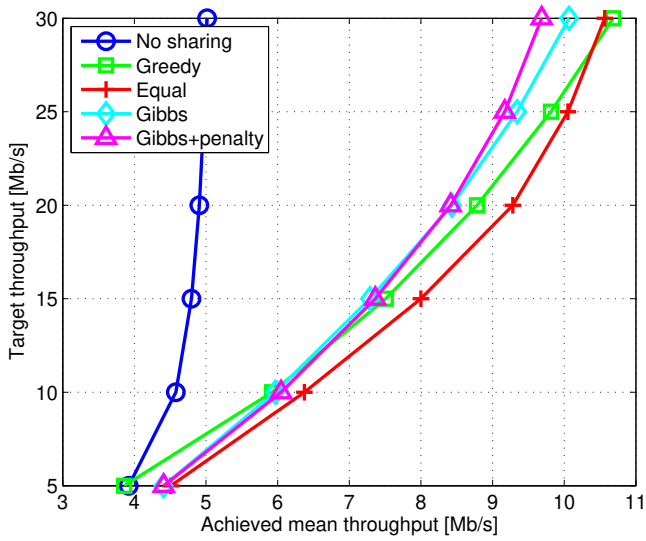

Fig. 28. Comparison of the different CoPSS algorithms for MNO1 when the downlink target throughput is increased.

algorithm is used. Finally, Fig. 30 reveals that if the Greedy algorithm is used for MNO2 and MNO3 with low data rate targets, the achieved performance gets worse than in the No sharing case while both Gibbs algorithms can achieve throughputs close to the Equal sharing, which is the best for this situation.

In Fig. 31 we present the Jain's index of the whole network. Fig. 31 shows that the Equal sharing algorithm provides the highest fairness in the network while the Gibbs with penalty can achieve fairness that is very close to it. When all the results are analyzed together we can conclude that the Gibbs with penalty algorithm can provide a considerably high throughput while ensuring fairness between the MNOs.

4.3.4 Performance results in random layout

The different CoPSS algorithms were analyzed by comparing the mean achieved rates. Fig. 32 shows the achieved mean throughput of MNO1 for different target rates. Here, we can capture how the CoPSS works when the MNOs have different throughput targets. In the simulations, we increase the MNO1 target throughput while MNO2 and MNO3 have a constant target throughput of 5 Mb/s. Note that, in the No sharing case, the

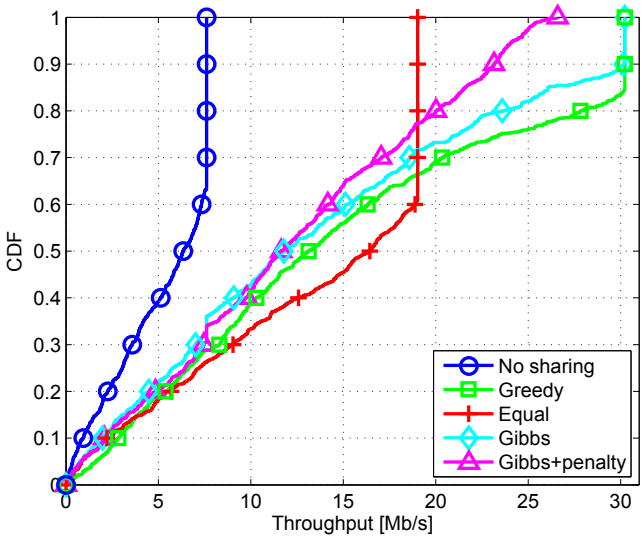

Fig. 29. The CDF of MNO1 downlink user throughput for different CoPSS algorithms when the target rate is 30 Mb/s.

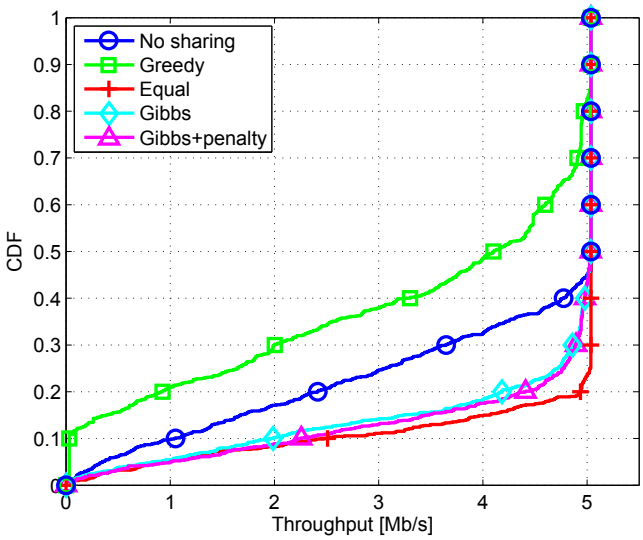

Fig. 30. The CDF of MNO2 and MNO3 downlink user throughput for different CoPSS algorithms when the target rate is 5 Mb/s.

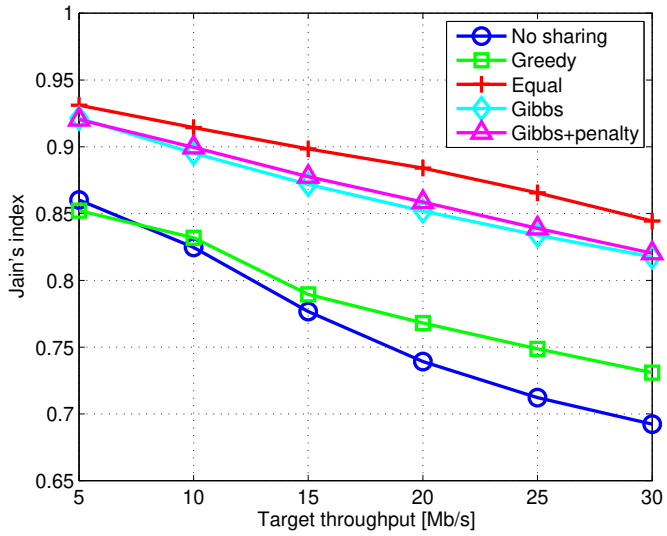

Fig. 31. Jain's index in the fixed network layout.

throughput saturates at around 5 Mb/s although the demand increases when the MNO cannot access the common pool of CCs. When the demand is low (5 – 15 Mb/s), the best achieved mean throughput is obtained with the different Gibbs and Equal algorithms while the Greedy algorithm provides the worst performance. When the demand increases (20 – 30 Mb/s), the Greedy algorithm provides better performance while the Equal algorithm starts to saturate. Furthermore, the Gibbs+distribution algorithm provides the overall best performance.

Fig. 33 shows the achieved mean throughput of MNO2&MNO3 for different target rates of MNO1. Again, the No sharing algorithm is still the worst, but also the Greedy algorithm exhibits poorer performance compared to the Equal and the Gibbs algorithms. For MNO2&MNO3, the best algorithm is the Gibbs+penalty algorithm because it is limits the number of CCs used by MNO1, and thus provides more free resources for MNO2&MNO3. The Gibbs+distribution algorithm is very close to the mean performance of the Gibbs+penalty algorithm. All the proposed Gibbs algorithms perform better than the Greedy or the Equal algorithm for MNO2&MNO3. In Fig. 34, the cumulative distribution function (CDF) of the throughput is analyzed when all the MNOs have the same throughput target of 5 Mb/s. The worst performances are achieved with the No sharing and the Greedy algorithms, and all the proposed Gibbs

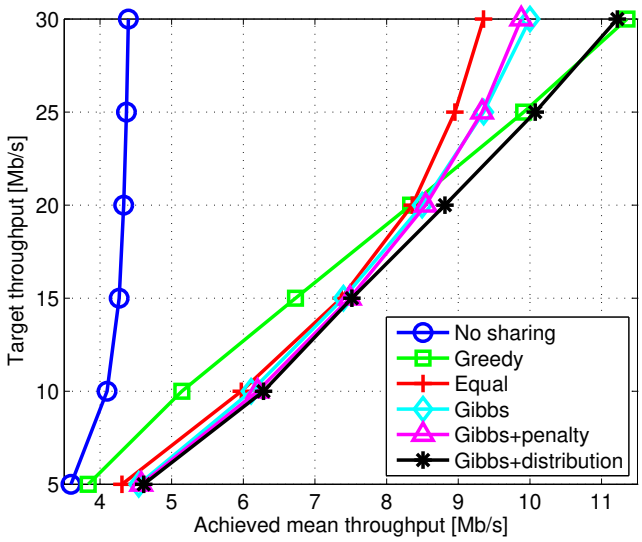

Fig. 32. Comparison of the different CoPSS algorithms for MNO1 when downlink target throughput for MNO1 is increased.

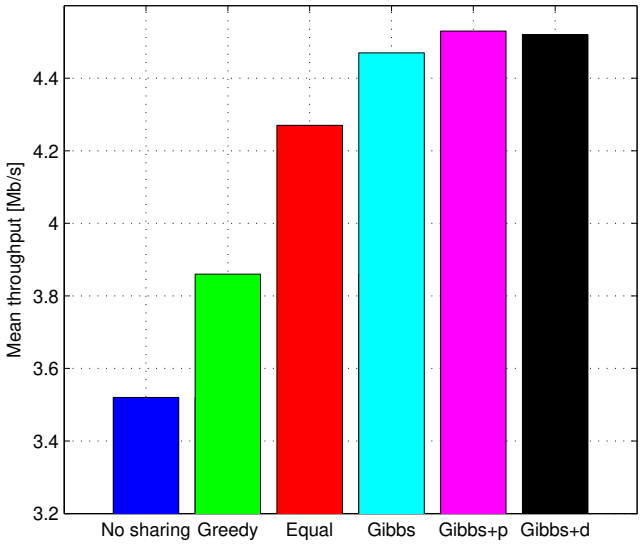

Fig. 33. Comparison of the different CoPSS algorithms for MNO2&MNO3 when downlink target throughput is 5 Mb/s.

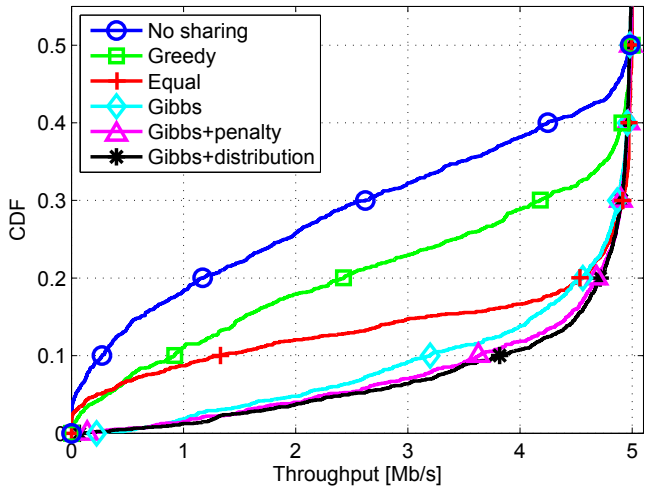

Fig. 34. The CDF of MNO1&MNO2&MNO3 downlink user throughput for different CoPSS algorithms when the target rate is 5 Mb/s.

Table 6. Cell edge user throughput [Mb/s] for MNO1&MNO2&MNO3 when the target rate is 5 Mb/s.

No sharing	Greedy	Equal	Gibbs	Gibbs+p	Gibbs+d
0.03	0.31	0.22	2.06	2.29	2.47

algorithms outperform the the Equal algorithm. The best performance is achieved with the Gibbs+distribution algorithm. When the cell edge (5% from CDFs) performance is analyzed, all the proposed algorithms outperform the state-of-the-art algorithms. The Gibbs+distribution offers almost 2.5 Mb/s better cell edge performance when compared to the state-of-art baselines that are in outage. Table 6 summarizes the achievable cell edge users' (5% from CDFs) throughputs for the different algorithms.

Figs. 35 and 36 show the CDF of the throughput for MNO1 with a 15 Mb/s target rate and MNO2&MNO3 with a 5 Mb/s target rate, respectively. For MNO1 the proposed Gibbs algorithms outperform the state-of-the-art algorithms. Moreover, throughputs for the cell edge can be vastly improved. The Gibbs+penalty provides 2 Mb/s while the Greedy and the Equal are in outage. For MNO2&MNO3, Fig. 36 shows similar performance to that in Fig. 34, but now the performance of the Greedy algorithm is even worse than in the previous case. Furthermore, the performance of the Gibbs algorithms is still at an acceptable level although there is a slight loss compared to the Equal

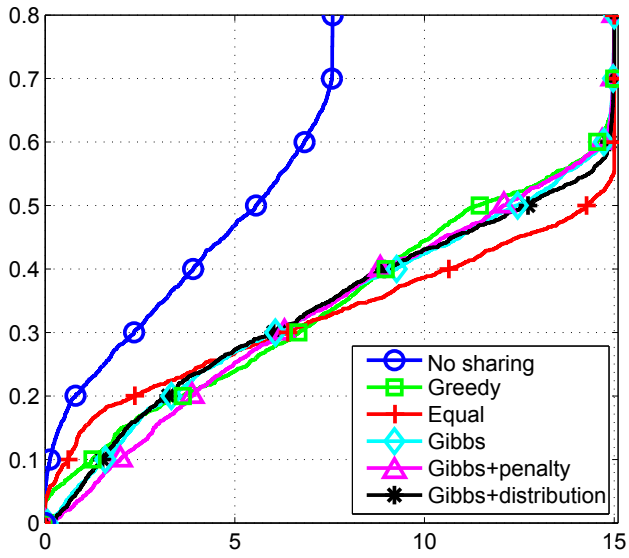

Fig. 35. The CDF of MNO1 downlink user throughput for different CoPSS algorithms when the target rate is 15 Mb/s.

Table 7. Cell edge user throughput [Mb/s] for MNO1 and MNO2&MNO3 when the target rate is 15 Mb/s and 5 Mb/s, respectively.

No sharing	Greedy	Equal	Gibbs	Gibbs+p	Gibbs+d
0	0.22	0.09	0.77	1.18	0.86
0.03	0.20	0.22	1.43	1.75	1.67

algorithm, and the cell edge throughput is much higher compared to the Equal algorithm. Table 7 summarizes the achievable cell edge users' (5% from CDFs) throughputs for the different algorithms.

In Fig. 37, we further increase MNO1 throughput demand to 30 Mb/s. Here, the Greedy provides the highest throughput, but still the cell edge is in outage. It can be seen that the Equal algorithm saturates at around 18 Mb/s, whereas the Gibbs and the Gibbs+penalty perform similar to the Equal algorithm from 4 Mb/s to 18 Mb/s. However, they can provide higher throughput for 30% of the users unlike the Equal algorithm. When the throughput demand is high, it is clear how the Gibbs+penalty algorithm is limiting the performance compared to the conventional Gibbs algorithm. When the conventional Gibbs achieves the target rate, the Gibbs+penalty provides 26

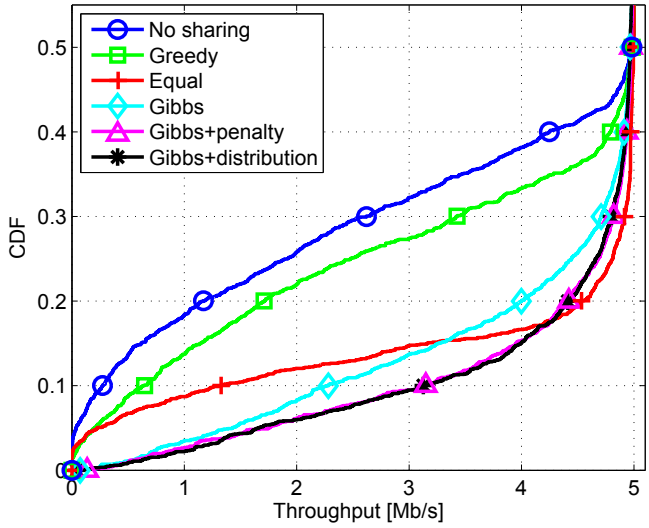

Fig. 36. The CDF of MNO2&MNO3 downlink user throughput for different CoPSS algorithms when the target rate is 5 Mb/s.

Table 8. Cell edge user throughput [Mb/s] for MNO1 and MNO2&MNO3 when the target rate is 30 Mb/s and 5 Mb/s, respectively.

No sharing	Greedy	Equal	Gibbs	Gibbs+p	Gibbs+d
0.01	0.04	0.02	0.66	1.17	0.83
0.06	0.19	0.33	0.88	1.27	0.71

Mb/s. In this scenario, the Gibbs+distribution achieves performance that is close to the Greedy algorithm while guaranteeing 2 Mb/s higher cell edge performance. As seen in Fig. 37, further increasing MNO1 throughput demand results performance degradation of MNO2&MNO3 that is close to the No sharing, when the Greedy algorithm is used. Here, the Gibbs+penalty algorithm provides the best cell edge and overall performance while the Gibbs and the Gibbs+distribution algorithms achieve slightly lower throughput, which is around 0.3 Mb/s. Table 8 summarizes the achievable cell edge users (5% from CDFs) throughputs for the different algorithms.

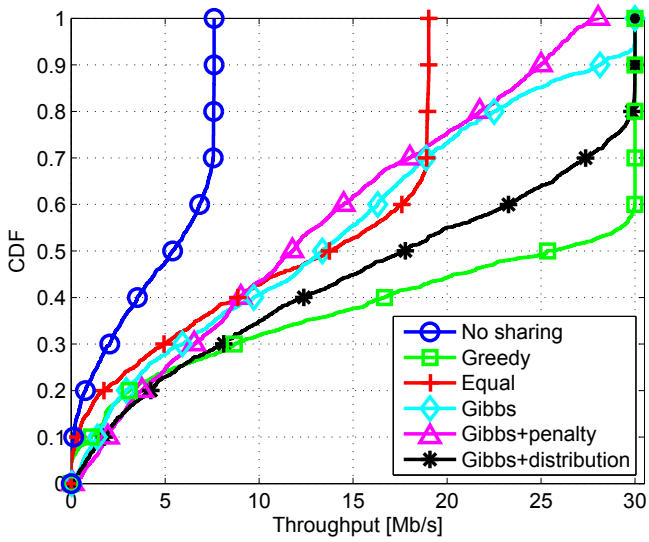

Fig. 37. The CDF of MNO1 downlink user throughput for different CoPSS algorithms when the target rate is 30 Mb/s.

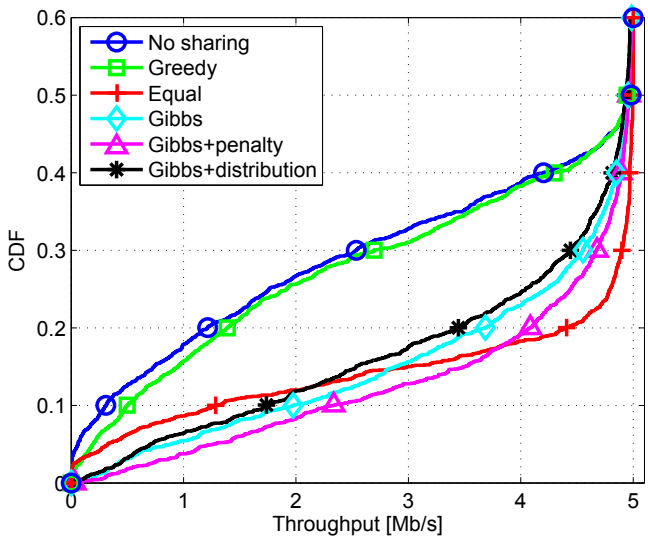

Fig. 38. The CDF of MNO2&MNO3 downlink user throughput for different CoPSS algorithms when the target rate is 5 Mb/s.

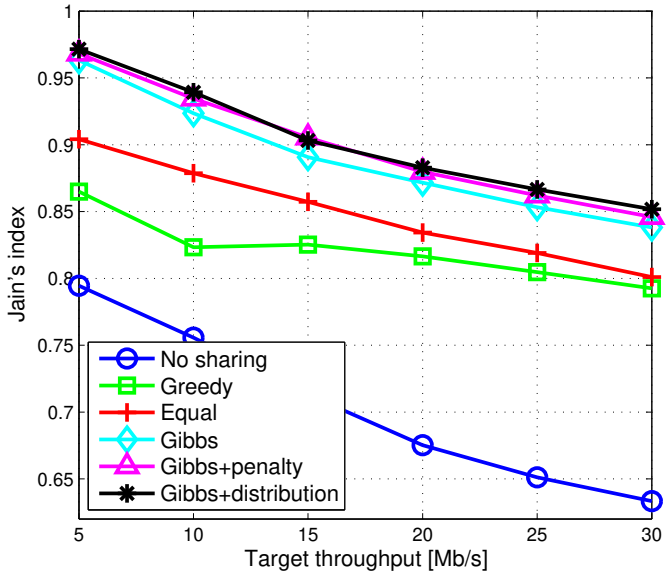

Fig. 39. Jain's index in the random network layout.

4.3.5 Fairness of spectrum sharing algorithms

Finally, in Fig. 39, we present the Jain's index of the whole network for different MNO1 demands and fixed 5 Mb/s for MNO2&MNO3. Fig. 39 shows that the Gibbs+distribution algorithm provides the highest fairness while the Gibbs+penalty is very close to it. All the proposed Gibbs algorithms outperform all of state-of-the-art baselines.

Analyzing all the results together, we can conclude that the Gibbs+distribution provides the best performance over state-of-the-art baselines. The proposed Gibbs+distribution algorithm provides higher utility, fairness and throughput. However, the Gibbs+penalty algorithm is suitable for scenarios, where MNOs need more control, especially over cell edge user throughputs. Although the proposed algorithms do not require continuous coordination between MNOs, still some level of coordination is needed. For instance, MNOs have to agree what is the pre-agreed maximum sharing ratio and the time window/penalty. However, the required amount of signaling for that is small and thus, the overhead is negligible.

4.3.6 Carrier frequency analysis

Due to higher cost and spectrum scarcity, it is expected that an efficient use of spectrum in fifth generation (5G) networks will rather rely on sharing than exclusive licenses, especially when higher frequency allocations are considered. Therefore, the spectrum sharing should be also analyzed at higher carrier frequency.

In the geometry-based stochastic channel model (GSCM), propagation channel is characterized by statistical parameters obtained from the radio channel measurements. This gives a possibility to use the same framework of the model for the simulations at different frequencies and the different number or types of antennas. Statistical parameters at 2 GHz have been taken from [106]. At 10 GHz, an indoor radio channel measurements have been carried out and the statistical parameters have been presented in [122].

Radio propagation channel behaves differently at different frequency bands. In general, path loss (PL) increases as the carrier frequency increases. However, due to shorter wavelength at 10 GHz, more antenna elements can be filled into the same space, making room to high gain antenna arrays to mitigate the increased path loss. Considering other channel model parameters at 10 GHz, delay spread and the angle spreads are smaller in [122] in comparison to the lower frequency band.

The main difference between propagation channel at 2 GHz and 10 GHz is the PL. Path loss models for indoor NLOS scenario at 2 GHz and 10 GHz are given by:

$$\mathrm{PL}_{@2\mathrm{GHz}} = 30\log_{10}(d) + 37 + A_{\mathrm{in}}k, \tag{30}$$

and

$$\mathrm{PL}_{@10\mathrm{GHz}} = 33\log_{10}(d) + 49.3 + A_{\mathrm{in}}k, \tag{31}$$

respectively. In (30) and (31) d is the distance in meters, A_{in} is the penetration loss of internal wall, and k is the number of penetrated walls. In general, the construction materials of the wall have significant impact on the penetration loss. Due to lack of internal wall penetration loss results at 10 GHz, we use the penetration loss of 10 dB for each internal wall.

Fig. 40 compares the path losses at 2 GHz and 10 GHz as a function of distance. Min and max distances are the minimum and maximum distances between a user and the SCN used in the simulations. Fig. 40 shows that there is 16 dB larger path loss for the higher carrier frequency.

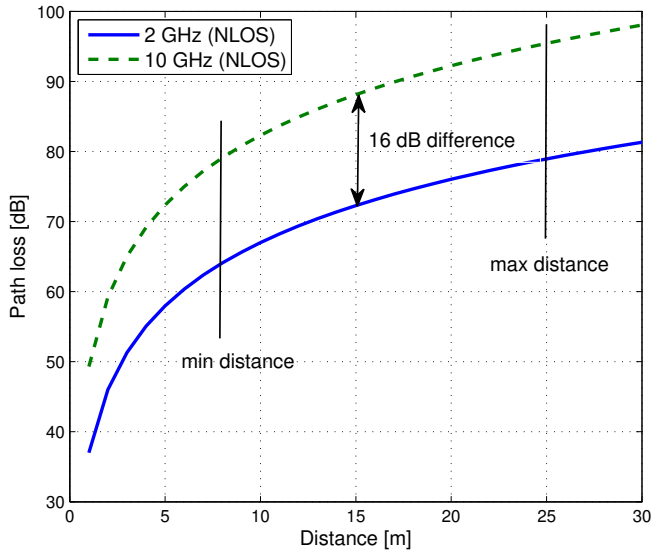

Fig. 40. Path loss (NLOS) comparison between 2 GHz and 10 GHz.

The mean received SINR at the two carrier frequencies and the CoPSS algorithms are analyzed in Fig. 41. First, we can see that the received SINR is higher at carrier frequency 2 GHz, particularly when SCN deployment probability η is low. The main reason is the higher path loss at 10 GHz carrier frequency. When η is increased, received SINR at 2 GHz carrier frequency decreases about 20 dB, while at 10 GHz, the decrease is only 10 dB. The reason is that the number of interfering SCNs in a dense network is much lower at the higher carrier frequency in comparison to the lower carrier frequency due to the higher path loss. From spectrum sharing point of view, Gibbs algorithm provides good SINR while the SINR of Greedy algorithm decreases rapidly as η increases. The reason is that Gibbs algorithm learns a suitable set of CCs in which the interference is minimized.

Next, in Fig. 42, we show the achieved mean throughput for the two carrier frequencies and the CoPSS algorithms. These results show that we can achieve higher throughput by applying the higher carrier frequency especially when network is dense, even though, the previous figure indicated that the received SINR is lower. The main reason is that the received SINR is not directly mapped to the achieved throughput (MIESM is used). Furthermore, the allocated resources can vary when different carrier

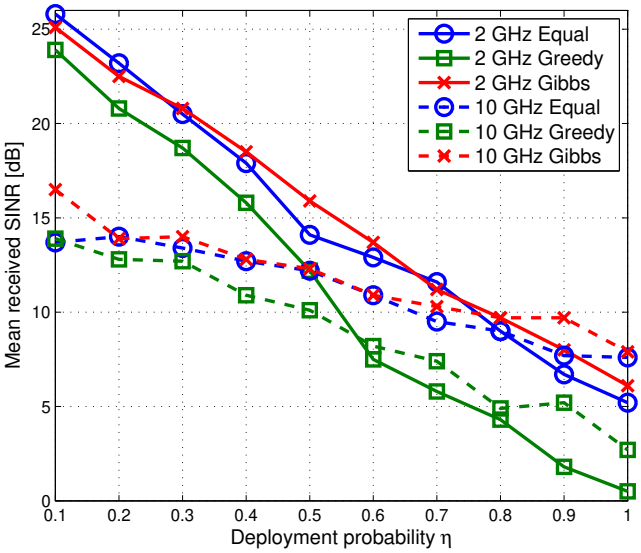

,

Fig. 41. Mean received SINR for different CoPSS algorithms and carrier frequencies when deployment probability is increased.

frequencies are used. The achieved performance with Equal algorithm is somewhat similar at both carrier frequencies because of the fixed spectrum allocation.

In Fig. 43, cumulative distribution function (CDF) of the throughput is analyzed when SCN deployment probability is 50%. At 10 GHz, the best overall performance is achieved. At the higher carrier frequency, the cell edge performance (5% of the CDF) is improved. Especially when Gibbs algorithm is used, the cell edge throughput is improved up to 2.0 Mb/s.

Table 9 summarizes the achievable cell edge users' (5% of the CDF) throughputs. It shows that when the carrier frequency is increased the cell edge throughput is increased. Furthermore, when $\eta = 100\%$, Equal and Greedy algorithms are in outage and only Gibbs algorithm provides throughput of 1.3 Mb/s at 10 GHz carrier frequency.

Analyzing all the results together, we can conclude that the higher carrier frequency can provide better performance and it allows denser networks. The CoPSS algorithm proposed in [87] is still the best one and the performance is even better at the higher carrier frequency.

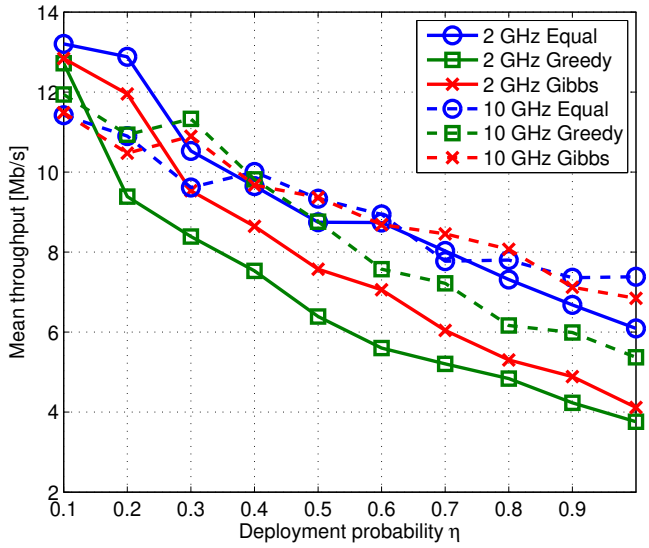

Fig. 42. Mean throughput for different CoPSS algorithms and carrier frequencies when deployment probability is increased.

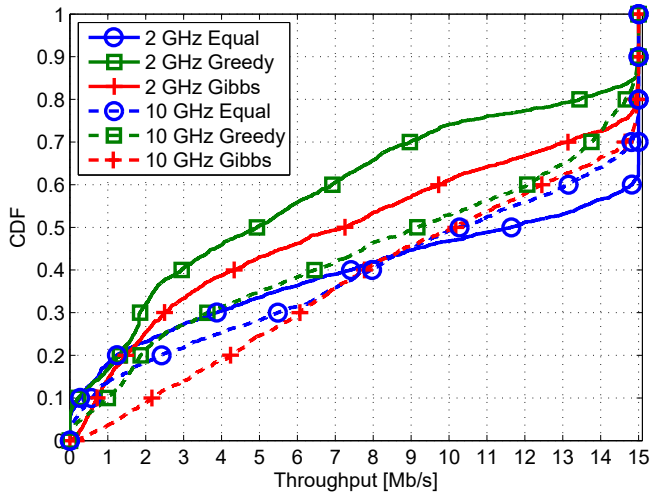

Fig. 43. CDF of downlink user throughput for different CoPSS algorithms and carrier frequencies when the target rate is 15 Mb/s, and SCN deployment probability is 50%.

Table 9. Cell edge user throughput for different deployment probabilities, carrier frequencies and CoPSS algorithms.

	$\eta = 10\%$		$\eta = 50\%$		$\eta = 100\%$	
	2 GHz	10 GHz	2 GHz	10 GHz	2 GHz	10 GHz
Equal	1.1	2.2	–	0.13	–	–
Greedy	1.9	1.8	–	0.33	–	–
Gibbs	5.5	2.7	0.6	1.2	0.1	1.3

4.4 Summary

In this chapter, we have evaluated five different approaches, two state-of-the art methods and three new algorithms for co-primary multi-operator spectrum sharing in a small cell indoor environment. A framework was established under a system simulation platform where the system throughput performance and fairness were rigorously assessed. We developed a decentralized control mechanism for base stations using the Gibbs sampling based learning tool, which allocates a suitable amount of spectrum for each base station while avoiding interference between SCNs and maximizing the total network throughput. Furthermore, we proposed distribution update initialization together with Gibbs sampling, which is possible with accurate CQI estimation.

Numerical results confirm the potential for co-primary spectrum sharing to increase system throughput in a multi-operator setting when mobile network operators share a common pool of component carriers. The results show that learning based algorithms without any coordination between small cell base stations can be used to efficiently share the spectrum, and these algorithms outperform state-of-the-art baselines. The proposed algorithms are suitable for operators with heterogeneous traffic requirements. The proposed algorithms significantly improve especially the cell edge performance. Moreover, the provided numerical results confirm the possibility for network densification when a higher carrier frequency is used and at the same time to further increase the system throughput.

5 Conclusions and future work

This thesis has proposed several co-primary spectrum sharing (CoPSS)algorithms for a multi-operator small cell network where mobile network operators (MNOs) share frequency bands. In the fifth generation (5G) networks it is expected that MNOs will rely on spectrum sharing rather than exclusive licenses. This is particularly viable at beyond 6 GHz carrier frequencies where the MNOs do not yet have usage. The proposed spectrum sharing methods are summarized as follows.

In Chapter 3, the idea of the proposed CoPSS algorithms is that the spectrum is shared orthogonally and equally between operators. This way interference can be avoided and spectrum utilization is maximized. In the three proposed algorithms, unused resources are shared equally between overloaded MNOs for a given time instant and the short term fairness among overloaded SCNs can be guaranteed. However, the long-term fairness (i.e., the equal amount of the average loaned/rented spectrum usage over a given time period) between MNOs cannot be guaranteed.

In Chapter 4, the MNOs share a common pool of radio resources. Moreover, the goal is to ensure the long term fairness of spectrum sharing without coordination between small cell base stations. We develop a decentralized control mechanism for the base stations using the Gibbs sampling based learning technique, which allocates a suitable amount of spectrum for each base station. We propose three decentralized algorithms (Gibbs, Gibbs+penalty and Gibbs+distribution) for CoPSS and compare them with three state-of-art algorithms (No sharing, Greedy and Equal).

In this thesis, different CoPSS approaches for mobile networks are comprehensively analyzed. The provided numerical results confirm the high potential of CoPSS to increase system throughput in the multi-operator setting. The results reveal the utmost importance of channel quality signaling between MNOs in order to take full advantage of the shared resources when MNOs are willing to share their dedicated spectrum. Furthermore, the results show that learning based algorithms without any coordination between small cell base stations can be used when the MNOs share a common pool of radio resources. The proposed learning based algorithms outperform the state-of-the-art baselines and they are suitable for operators with heterogeneous traffic requirements. The cell edge performance especially is significantly improved. The proposed algorithms are shown to be effective for different network layouts, by achieving significant data

rate enhancements with low overheads. Furthermore, MNOs have to share a minimal amount of operator-specific information or have no information exchange at all.

In future work, spectrum sharing could be done over network slicing, which would enable a much more efficient sharing of network resources. In this approach the idea would be to provide networks on an as-a-service basis and meet a wide range of use cases. Network slicing is an important feature of the future 5G network because the use cases will be highly diverse varying from very high data rate connections to low data rate massive machine-type communication (MTC). Each use case has different requirements and network parameters. The network is built in a flexible way so that network parameters can be optimized for each service. In order to slice the network software defined networking (SDN) approaches are needed together with network function virtualization (NFV).

The idea of network slicing also enables the possibility to use micro operators, where property owners use local networks to provide specific, localized services for public buildings, shopping malls or industrial sites. This allows micro operators to locally control the network and provide the best local services required in that venue. For example, a shopping mall micro operator could offer free connectivity to all visitors, while having targeted advertisements for the visitors.

Another promising future topic is dynamic time division duplexing (TDD) especially for 5G small cell networks. Dynamic TDD is attractive for SCNs because a small number of simultaneously active users per cell and SCNs typically do not inflict significant interference on each other. The idea is to drastically improve data rates by adapting the TDD pattern based on the user traffic direction.

References

1. Chen S & Zhao J (2014) The requirements, challenges, and technologies for 5G of terrestrial mobile telecommunication. IEEE Communications Magazine 52(5): 36–43.
2. Hossain E, Rasti M, Tabassum H & Abdelnasser A (2014) Evolution toward 5G multi-tier cellular wireless networks: An interference management perspective. IEEE Wireless Communications 21(3): 118–127.
3. Dahlman E, Mildh G, Parkvall S, Peisa J, Sachs J, Selén Y & Sköld J (2014) 5G wireless access: requirements and realization. IEEE Communications Magazine 52(12): 42–47.
4. Fettweis G & Alamouti S (2014) 5G: Personal mobile internet beyond what cellular did to telephony. IEEE Communications Magazine 52(2): 140–145.
5. Nokia, 5G use cases and requirements. URI: http://resources.alcatel-lucent.com/asset/200010.
6. Ericsson, 5G radio access research and vision. URI: http://www.ericsson.com/news/130625-5g-radio-access-research-and-vision.
7. Gupta A & Jha RK (2015) A survey of 5G network: Architecture and emerging technologies. IEEE Access 3: 1206–1232.
8. Ericsson, Challenges for 2020 and beyond. URI: http://www.ericsson.com/res/docs/whitepapers/wp-5g.pdf.
9. METIS. URI: https://www.metis2020.com/.
10. Zhang J & de la Roche G (2010) Femtocells: Technologies and Deployment.
11. Huawei Technologies Co., Ltd. (2013) LTE Small Cell v.s. WiFi User Experience.
12. Nokia, small cells - adding capacity at low cost. URI: https://networks.nokia.com/sites/content/files/small-cells-1.jpg.
13. Wang Y, Li J, Huang L, Jing Y, Georgakopoulos A & Demestichas P (2014) 5g mobile: Spectrum broadening to higher-frequency bands to support high data rates. IEEE Vehicular Technology Magazine 9(3): 39–46.
14. Merz P (2014) Nokia, Optimising Spectrum Utilisation towards 2020 URI: https://johannesbergsummit.com/wp-content/uploads/sites/6/2013/11/Merz-Optimizing-Spectrum-Usage-for-2020-and-Beyond-Johannesberg-Summit-2014-Peter-Merz.pdf.
15. METIS deliverable D5.1 Intermediate description of the spectrum needs and usage principles. URI: https://www.metis2020.com/documents/deliverables/.
16. Irnich T, Kronander J, Selén Y & Li G (2013) Spectrum sharing scenarios and resulting technical requirements for 5G systems. In: IEEE 24th International Symposium on Personal, Indoor and Mobile Radio Communications (PIMRC Workshops), pp. 127–132.
17. USA TODAY, FCC approves spectrum for 5G advances. URI: http://www.usatoday.com/story/tech/news/2016/07/14/fcc-approves-spectrum-5g-advances/87081242/.
18. Singh B, Koufos K & Tirkkonen O (2014) Co-primary inter-operator spectrum sharing using repeated games. In: IEEE International Conference on Communication Systems (ICCS), pp. 67–71.
19. Electronic Communications Committee, ECC report 132, light licensing, licence-exempt and commons .
20. RSPG. RSPG opinion on licensed shared access, RSPG13-538, European Commission, Radio Spectrum Policy Group, Nov 2013.

21. Dahlman E, Parkvall S & Sköld J (2011) 4G: LTE/LTE-Advanced for Mobile Broadband. Elsevier Science.
22. Hamza AS, Khalifa SS, Hamza HS & Elsayed K (2013) A survey on inter-cell interference coordination techniques in OFDMA-based cellular networks. IEEE Communications Surveys Tutorials 15(4): 1642–1670.
23. Rangan S (2010) Femto-macro cellular interference control with subband scheduling and interference cancelation. In: 2010 IEEE Globecom Workshops, pp. 695–700.
24. Vorobyov SA, Gershman AB & Luo ZQ (2003) Robust adaptive beamforming using worst-case performance optimization: a solution to the signal mismatch problem. IEEE Transactions on Signal Processing 51(2): 313–324.
25. Liang YS, Chung WH, Ni GK, Chen IY, Zhang H & Kuo SY (2012) Resource allocation with interference avoidance in ofdma femtocell networks. IEEE Transactions on Vehicular Technology 61(5): 2243–2255.
26. Kim T, Lee S, Chhorn S, Cho C & Ryu S (2012) Resource allocation and power control scheme for interference avoidance in LTE-Advanced device-to-device communication. In: 7th International Conference on Computing and Convergence Technology (ICCCT), pp. 1201–1204.
27. Lai WS, Chiang ME, Lee SC & Lee TS (2013) Game theoretic distributed dynamic resource allocation with interference avoidance in cognitive femtocell networks. In: 2013 IEEE Wireless Communications and Networking Conference (WCNC), pp. 3364–3369.
28. Tehrani RH, Vahid S, Triantafyllopoulou D, Lee H & Moessner K (2016) Licensed spectrum sharing schemes for mobile operators: A survey and outlook. IEEE Communications Surveys Tutorials pp(99): 1–1.
29. Spapis P, Chatzikokolakis K, Alonistioti N & Kaloxylos A (2014) Using SDN as a key enabler for co-primary spectrum sharing. In: The 5th International Conference on Information, Intelligence, Systems and Applications, (IISA), pp. 366–371.
30. Yu Q, Wang J, Yang X, Zhu Y, Teng Y & Horneman K (2015) Inter-operator interference coordination for co-primary spectrum sharing in UDN. China Communications 12(Supplement): 104–112.
31. Cho B, Koufos K, Jäntti R, Li Z & Uusitalo MA (2015) Spectrum allocation for multi-operator device-to-device communication. In: 2015 IEEE International Conference on Communications (ICC), pp. 5454–5459.
32. Dahlberg C, Liu Z, Pradini A & Sung KW (2013) A techno-economic framework of spectrum combining for indoor capacity provisioning. In: 2013 IEEE 24th Annual International Symposium on Personal, Indoor, and Mobile Radio Communications (PIMRC), pp. 2759–2763.
33. Qualcomm Authorized Shared Access (ASA), Enabling more spectrum. URI: https://www.qualcomm.com/invention/research/projects/lte-advanced/asa.
34. Mustonen M, Chen T, Saarnisaari H, Matinmikko M, Yrjola S & Palola M (2014) Cellular architecture enhancement for supporting the European licensed shared access concept. IEEE Wireless Communications 21(3): 37–43.
35. Matinmikko M, Mustonen M, Roberson D, Paavola J, Höyhtyä M, Yrjölä S & Röning J (2014) Overview and comparison of recent spectrum sharing approaches in regulation and research: From opportunistic unlicensed access towards licensed shared access. In: IEEE International Symposium on Dynamic Spectrum Access Networks (DYSPAN), pp. 92–102.

36. Wireless Innovation Forum, Requirements for commercial operation in the U.S. 3550-3700 MHz citizens broadband radio service band, WINNF-15-S-0112 V1.0.0.
37. Reed JH, Clegg AW, Padaki AV, Yang T, Nealy R, Dietrich C, Anderson CR & Mearns DM (2016) On the co-existence of TD-LTE and radar over 3.5GHz band: An experimental study (99): 1–1.
38. Ghorbanzadeh M, Visotsky E, Moorut P, Yang W & Clancy C (2015) Radar inband and out-of-band interference into LTE macro and small cell uplinks in the 3.5GHz band. pp. 1829–1834.
39. Ghorbanzadeh M, Visotsky E, Moorut P, Yang W & Clancy C (2016) Radar interference into LTE base stations in the 3.5GHz band pp. 33–47.
40. Shajaiah H, Abdelhadi A & Clancy C (2015) Spectrum sharing approach between radar and communication systems and its impact on radar's detectable target parameters. pp. 1–6.
41. ITU Global Symposium for Regulators, Capitalizing on the potential of the digital worlds URI: http://www.itu.int/en/ITU-R/workshops/Pre-GSR-14/Presentations/2-IEEE%20TVWS-2014-V3.pdf.
42. SAPHYRE Project, Deliverable D7.2c, 2013, regulation and standardisation plan.
43. ETSI, Work programme 2014-2015, Building the future, White Paper, Jun. 2014.
44. Study on Radio Access Network (RAN) sharing enhancements, 3GPP TR 22.852 V13.1.0, Sep. 2014.
45. Network Sharing Architecture and functional description, 3GPP TS 23.251 V13.1.0, Mar. 2015.
46. Sharing Physical Resources Mechanisms and Implementations for Wireless Networks (SAPHYRE). URI: http://www.saphyre.eu/index.html.
47. Katzela I & Naghshineh M (1996) Channel assignment schemes for cellular mobile telecommunication systems: a comprehensive survey. IEEE Personal Communications 3(3): 10–31.
48. Salami G, Durowoju O, Attar A, Holland O, Tafazolli R & Aghvami H (2011) A comparison between the centralized and distributed approaches for spectrum management. IEEE Communications Surveys Tutorials 13(2): 274–290.
49. Xu Y, Anpalagan A, Wu Q, Shen L, Gao Z & Wang J (2013) Decision-theoretic distributed channel selection for opportunistic spectrum access: Strategies, challenges and solutions. IEEE Communications Surveys Tutorials 15(4): 1689–1713.
50. Masonta MT, Mzyece M & Ntlatlapa N (2013) Spectrum decision in cognitive radio networks: A survey. IEEE Communications Surveys Tutorials 15(3): 1088–1107.
51. Tragos EZ, Zeadally S, Fragkiadakis AG & Siris VA (2013) Spectrum assignment in cognitive radio networks: A comprehensive survey. IEEE Communications Surveys Tutorials 15(3): 1108–1135.
52. Paisana F, Marchetti N & DaSilva LA (2014) Radar, TV and cellular bands: Which spectrum access techniques for which bands? IEEE Communications Surveys Tutorials 16(3): 1193–1220.
53. Tsiropoulos GI, Dobre OA, Ahmed MH & Baddour KE (2016) Radio resource allocation techniques for efficient spectrum access in cognitive radio networks. IEEE Communications Surveys Tutorials 18(1): 824–847.
54. Leaves P, Ghaheri-Niri S, Tafazolli R, Christodoulides L, Sammut T, Staht W & Huschke J (2001) Dynamic spectrum allocation in a multi-radio environment: concept and algorithm. In: Second International Conference on 3G Mobile Communication Technologies, 2001.(Conf.

Publ. No. 477), pp. 53–57.
55. Salgado H, Sirbu M & Peha J (1995) Spectrum sharing through dynamic channel assignment for open access to personal communications services. In: IEEE International Conference on Communications (ICC), volume 1, pp. 417–422 vol.1.
56. Alsohaily A & Sousa ES (2013) Performance gains of spectrum sharing in multi-operator LTE-Advanced systems. In: IEEE 78th Vehicular Technology Conference (VTC Fall), pp. 1–5.
57. Alsohaily A & Sousa ES (2014) Dynamic spectrum access for multi-radio access technology, multi-operator autonomous small cell communication systems. In: IEEE 25th Annual International Symposium on Personal, Indoor, and Mobile Radio Communication (PIMRC), pp. 1778–1782.
58. Han S, Liang YC & Soong BH (2015) Spectrum refarming: A new paradigm of spectrum sharing for cellular networks. IEEE Transactions on Communications 63(5): 1895–1906.
59. Aazhang B, Lilleberg J & Middleton G (2004) Spectrum sharing in a cellular system. In: IEEE Eighth International Symposium on Spread Spectrum Techniques and Applications, pp. 355–359.
60. Bennis M & Lilleberg J (2006) Inter-operator resource sharing for 3G systems and beyond. In: IEEE Ninth International Symposium on Spread Spectrum Techniques and Applications, pp. 401–405.
61. Mazzenga F, Petracca M, Pomposini R, Vatalaro F & Giuliano R (2011) Performance evaluation of spectrum sharing algorithms in single and multi operator scenarios. In: IEEE 73rd Vehicular Technology Conference (VTC Spring), pp. 1–5.
62. Jorswieck E, Badia L, Fahldieck T, Karipidis E & Luo J (2014) Spectrum sharing improves the network efficiency for cellular operators. IEEE Communications Magazine 52(3): 129–136.
63. Panchal J, Yates R & Buddhikot M (2013) Mobile network resource sharing options: Performance comparisons. IEEE Transactions on Wireless Communications 12(9): 4470–4482.
64. Sanguanpuak T, Guruacharya S, Rajatheva N & Latva-Aho M (2015) Resource allocation for co-primary spectrum sharing in MIMO networks. In: 2015 IEEE International Conference on Communication Workshop (ICCW), pp. 1083–1088.
65. Sanguanpuak T, Rajatheva N & Latva-aho M (2014) Co-primary spectrum sharing with resource allocation in small cell network. In: 1st International Conference on 5G for Ubiquitous Connectivity (5GU), pp. 6–10.
66. Teng Y, Wang Y & Horneman K (2014) Co-primary spectrum sharing for denser networks in local area. In: 9th International Conference on Cognitive Radio Oriented Wireless Networks and Communications (CROWNCOM), pp. 120–124.
67. Singh B, Koufos K, Tirkkonen O & Berry R (2015) Co-primary inter-operator spectrum sharing over a limited spectrum pool using repeated games. In: 2015 IEEE International Conference on Communications (ICC), pp. 1494–1499.
68. Singh B, Hailu S, Koufos K, Dowhuszko A, Tirkkonen O, Jäntti R & Berry R (2015) Coordination protocol for inter-operator spectrum sharing in co-primary 5G small cell networks. IEEE Communications Magazine 53(7): 34–40.
69. Hailu S, Dowhuszko AA & Tirkkonen O (2014) Adaptive co-primary shared access between co-located radio access networks. In: 2014 9th International Conference on Cognitive Radio Oriented Wireless Networks and Communications (CROWNCOM), pp. 131–135.

70. Hailu S, Dowhuszko AA, Tirkkonen O & Wei L (2014) One-shot games for spectrum sharing among co-located radio access networks. In: IEEE International Conference on Communication Systems (ICCS), pp. 61–66.
71. Syed AR & Yau KLA (2014) Spectrum leasing in cognitive radio networks: A survey. International Journal of Distributed Sensor Networks 10(2). URI: http://dsn.sagepub.com/content/10/2/329235.abstract.
72. Bajaj I, Lee YH & Gong Y (2015) A spectrum trading scheme for licensed user incentives. IEEE Transactions on Communications 63(11): 4026–4036.
73. Simeone O, Stanojev I, Savazzi S, Bar-Ness Y, Spagnolini U & Pickholtz R (2008) Spectrum leasing to cooperating secondary ad hoc networks. IEEE Journal on Selected Areas in Communications 26(1): 203–213.
74. Zhou X & Zheng H (2009) TRUST: A general framework for truthful double spectrum auctions. In: IEEE INFOCOM, pp. 999–1007.
75. Jayaweera SK & Li T (2009) Dynamic spectrum leasing in cognitive radio networks via primary-secondary user power control games. IEEE Transactions on Wireless Communications 8(6): 3300–3310.
76. Jayaweera SK, Vazquez-Vilar G & Mosquera C (2010) Dynamic spectrum leasing: A new paradigm for spectrum sharing in cognitive radio networks. IEEE Transactions on Vehicular Technology 59(5): 2328–2339.
77. Ahokangas P, Horneman K, Posti H, Matinmikko M, Hänninen T, Yrjölä S & Goncalves V (2014) Defining co-primary spectrum sharing, A new business opportunity for MNOs? In: 9th International Conference on Cognitive Radio Oriented Wireless Networks and Communications (CROWNCOM), pp. 395–400.
78. Ahokangas P, Horneman K, Matinmikko M, Yrjölä S, Posti H & Okkonen H (2016) Co-primary spectrum sharing and its impact on MNOs' business model scalability, pp. 695–702. Springer International Publishing, Cham.
79. Dahlberg C, Liu Z, Pradini A & Sung KW (2013) A techno-economic framework of spectrum combining for indoor capacity provisioning. In: 2013 IEEE 24th Annual International Symposium on Personal, Indoor, and Mobile Radio Communications (PIMRC), pp. 2759–2763.
80. Ahokangas P, Matinmikko M, Yrjölä S, Mustonen M, Posti H, Luttinen E & Kivimäki A (2014) Business models for mobile network operators in licensed shared access (LSA). In: IEEE International Symposium on Dynamic Spectrum Access Networks (DYSPAN), pp. 263–270.
81. Kang DH, Sung KW & Zander J (2013) High capacity indoor and hotspot wireless systems in shared spectrum: a techno-economic analysis. IEEE Communications Magazine 51(12): 102–109.
82. Ahokangas P, Matinmikko M, Yrjola S, Okkonen H & Casey T (2013) "Simple rules" for mobile network operators' strategic choices in future cognitive spectrum sharing networks. IEEE Wireless Communications 20(2): 20–26.
83. Hultell J, Johansson K & Markendahl J (2004) Business models and resource management for shared wireless networks. In: IEEE 60th Vehicular Technology Conference (VTC), pp. 3393–3397 Vol. 5.
84. Nokia Siemens Networks. Self-Organizing Network (SON), Introducing the Nokia Siemens Networks SON Suite - an efficient, future-proof platform for SON, (2009).

85. Luoto P, Pirinen P, Bennis M, Samarakoon S, Scott S & Latva-aho M (2015) Co-primary multi-operator resource sharing for small cell networks. IEEE Transactions on Wireless Communications 14(6): 3120–3130.
86. Luoto P, Pirinen P, Bennis M, Samarakoon S & Latva-aho M (2017) Enhanced co-primary spectrum sharing method for multi-operator networks. IEEE Transactions on Mobile Computing (conditionally accepted) .
87. Luoto P, Bennis M, Pirinen P, Samarakoon S & Latva-aho M (2015) Gibbs sampling based spectrum sharing for multi-operator small cell networks. In: IEEE International Conference on Communication Workshop (ICCW), pp. 967–972.
88. Luoto P, Roivainen A, Bennis M, Pirinen P, Samarakoon S & Latva-aho M (2017) System level analysis of multi-operator small cell network at 10 GHz. In: EuCNC (submitted).
89. Newman MEJ (2003) The structure and function of complex networks. SIAM REVIEW 45: 167–256.
90. Mach P & Becvar Z (2014) Centralized dynamic resource allocation scheme for femtocells exploiting graph theory approach. In: 2014 IEEE Wireless Communications and Networking Conference (WCNC), pp. 1479–1484.
91. Hu P, Ye J, Zhang F, Deng S, Wang C & Wang W (2012) Downlink resource management based on cross-cognition and graph coloring in cognitive radio femtocell networks. In: Vehicular Technology Conference (VTC Fall), 2012 IEEE, pp. 1–5.
92. Uygungelen S, Auer G & Bharucha Z (2011) Graph-based dynamic frequency reuse in femtocell networks. In: IEEE 73rd Vehicular Technology Conference (VTC Spring), pp. 1–6.
93. Uygungelen S & Bharucha Z (2012) A dynamic resource assignment method for uncoordinated wireless networks. In: IEEE Vehicular Technology Conference (VTC Fall), pp. 1–6.
94. Ruohonen K (2013) MAT-62756 Graph theory. Tampere University of Technology.
95. Formanowicz P & Tanas K (2012) A survey of graph coloring - its types, methods and applications,. Foundations of Computing and Decision Sciences. 37(3): 223–238.
96. Yuille AL & Grzywacz NM (1988) The motion coherence theory. In: Second International Conference on Computer Vision,, pp. 344–353.
97. von Luxburg U (2007) A tutorial on spectral clustering. CoRR abs/0711.0189. URI: http://arxiv.org/abs/0711.0189.
98. Tesauro G, Jong NK, Das R & Bennani MN (2006) A hybrid reinforcement learning approach to autonomic resource allocation. In: 2006 IEEE International Conference on Autonomic Computing, pp. 65–73.
99. Perlaza SM, Tembine H & Lasaulce S (2010) How can ignorant but patient cognitive terminals learn their strategy and utility? In: Signal Processing Advances in Wireless Communications (SPAWC), IEEE Eleventh International Workshop on, pp. 1–5.
100. Bennis M & Perlaza SM (2011) Decentralized cross-tier interference mitigation in cognitive femtocell networks. In: 2011 IEEE International Conference on Communications (ICC), pp. 1–5.
101. Iacoboaiea O, Sayrac B, Jemaa SB & Bianchi P (2014) Coordinating son instances: A reinforcement learning framework. In: 2014 IEEE 80th Vehicular Technology Conference (VTC2014-Fall), pp. 1–5.
102. Iacoboaiea OC, Sayrac B, Jemaa SB & Bianchi P (2016) SON coordination in heterogeneous networks: A reinforcement learning framework. IEEE Transactions on Wireless

Communications 15(9): 5835–5847.
103. Khosrowpour M & Association IRM (2012) Machine Learning: Concepts, Methodologies, Tools and Applications. Number nid. 1 in Machine Learning: Concepts, Methodologies, Tools and Applications. Information Science Reference. URI: https://books.google.fi/books?id=9j5KYgEACAAJ.
104. Brémaud P (1999) Markov Chains: Gibbs Fields Monte Carlo Simulation and Queues. Springer Science & Busines Media.
105. BeFEMTO. Assumptions For System Level Calibration. Version 0.8, Mar. 2011.
106. WINNER II channel models, D1.1.2 V1.2.
107. 3rd Generation Partnership Project, Technical Specification Group Radio Access Network, Spatial channel model for Multiple Input Multiple Output (MIMO) simulations, 3GPP Technical report 25.996 v6.1.0.
108. He X, Niu K, He Z & Lin J (2007) Link layer abstraction in MIMO-OFDM system. In: International Workshop on Cross Layer Design (IWCLD), pp. 41–44.
109. Guidelines for evaluation of radio interface technologies for IMT-Advanced, Report ITU-R M.2135-1.
110. MATLAB implementation of the WINNER Phase II Channel Model ver1.1. URI: https://www.ist-winner.org/phase_2_model.html.
111. Pennanen H, Haataja T, Leinonen J, Tölli A & Latva-aho M (2010) System level evaluation of TDD based LTE-Advanced MIMO-OFDMA systems. In: IEEE GLOBECOM Workshops (GC Wkshps), pp. 809–813.
112. Haataja T, Pennanen H, Leinonen J, Tölli A & Latva-aho M (2011) Space-frequency scheduling in TDD based LTE-Advanced MIMO-OFDMA systems. In: IEEE 73rd Vehicular Technology Conference (VTC Spring), pp. 1–5.
113. BeFEMTO URI: http://www.ict-befemto.eu/home.html.
114. Luoto P, Leinonen J, Pirinen P, Phan VV & Latva-aho M (2013) Bit-map based resource partitioning in LTE-A femto deployment. In: IEEE International Conference on Communications (ICC), pp. 5005–5009.
115. Luoto P, Pirinen P & Latva-aho M (2013) Energy efficient load sharing in LTE-A hetnets. In: IEEE 9th International Conference on Wireless and Mobile Computing, Networking and Communications (WiMob), pp. 119–123.
116. Kokkoniemi J, Ylitalo J, Luoto P, Scott S, Leinonen J & Latva-aho M (2013) Performance evaluation of vehicular lte mobile relay nodes. In: IEEE 24th Annual International Symposium on Personal, Indoor, and Mobile Radio Communications (PIMRC), pp. 1972–1976.
117. Luoto P, Bennis M, Pirinen P, Samarakoon S, Horneman K & Latva-aho M (2016) System level performance evaluation of LTE-V2X network. In: 22th European Wireless Conference, pp. 1–5.
118. Luoto P, Bennis M, Pirinen P, Samarakoon S, Horneman K & Latva-aho M (2017) LTE-V2X network performance improvement with spectral clustering. In: EuCNC (submitted).
119. Qian LP, YJA Z & Chiang M (2012) Distributed nonconvex power control using Gibbs sampling. IEEE Transactions on Communications 60(12): 3886–3898.
120. Borst S, Markakis M & Saniee I (2014) Nonconcave utility maximization in locally coupled systems, with applications to wireless and wireline networks. IEEE/ACM Transactions on Networking 22(2): 674–687.

121. Jain R, Chiu D & Hawe W (1998) A quantitative measure of fairness and discrimination for resource allocation in shared computer systems. CoRR .
122. Roivainen A, Ferreira Dias C, Tervo N, Hovinen V, Sonkki M & Latva-aho M (2016) Geometry-based stochastic channel model for two-story lobby environment at 10 GHz. IEEE Transactions on Antennas and Propagations. 64(9): 3990–4003.

588. Varjo, Sami (2016) A direct microlens array imaging system for microscopy

589. Haapakangas, Juho (2016) Coke properties in simulated blast furnace conditions : investigation on hot strength, chemical reactivity and reaction mechanism

590. Erkkilä-Häkkinen, Sirpa (2016) Rakentamisen työturvallisuuteen suhtautuminen toimijoiden kokemuksina

591. Hassani Nezhad Gashti, Ehsan (2016) Thermo-mechanical behaviour of ground-source thermo-active structures

592. Sulasalmi, Petri (2016) Modelling of slag emulsification and slag reduction in CAS-OB process

593. Liyanage, Madhusanka (2016) Enhancing security and scalability of Virtual Private LAN Services

594. Darif, Bouchra (2016) Synthesis and characterization of catalysts used for the catalytic oxidation of sulfur-containing volatile organic compounds : focus on sulfur-induced deactivation

595. Juholin, Piia (2016) Hybrid membrane processes in industrial water treatment : separation and recovery of inorganic compounds

596. Augustine, Bobins (2016) Efficiency and stability studies for organic bulk heterojunction solar cells

597. Ylioinas, Juha (2016) Towards optimal local binary patterns in texture and face description

598. Mohammadighavam, Shahram (2017) Hydrological and hydraulic design of peatland drainage and water treatment systems for optimal control of diffuse pollution

599. Louis, Jean-Nicolas (2016) Dynamic environmental indicators for smart homes : assessing the role of home energy management systems in achieving decarbonisation goals in the residential sector

600. Mustamo, Pirkko (2017) Greenhouse gas fluxes from drained peat soils : a comparison of different land use types and hydrological site characteristics

601. Upola, Heikki (2017) Disintegration of packaging material : an experimental study of approaches to lower energy consumption

603. Kokkoniemi, Joonas (2017) Nanoscale sensor networks: The THz band as a communication channel

Book orders:
Granum: Virtual book store
http://granum.uta.fi/granum/

UNIVERSITY OF OULU P.O. Box 8000 FI-90014 UNIVERSITY OF OULU FINLAND

ACTA UNIVERSITATIS OULUENSIS

UNIVERSITY of OULU
OULUN YLIOPISTO

ISBN 978-952-62-1496-2 (Paperback)
ISBN 978-952-62-1497-9 (PDF)
ISSN 0355-3213 (Print)
ISSN 1796-2226 (Online)